Inorganic Chemistry

FORUM ARTICLE

pubs.acs.org/IC

s-Block Organometallics: Analysis of Ion-Association and Noncovalent Interactions on Structure and Function in Benzyl-Based Compounds

Ana Torvisco and Karin Ruhlandt-Senge*

Department of Chemistry, Syracuse University, 1-014 CST, Syracuse, New York 13244, United States

ABSTRACT: The organometallic chemistry of alkali and alkaline-earth metals has been marred by synthetic setbacks because of their high reactivity. Advances in their synthesis and a better understanding of the stabilization effects of ligands and coligands have resulted in the revolution of s-block organometallics. Among those, benzyl-based derivatives have played a key role in developing this chemistry because factors such as the ligand size, charge delocalization, and introduction of electronic parameters along with metal effects can be analyzed. This article will focus on s-block benzylates and di- and triphenylmethanide derivatives with specific emphasis on the factors that stabilize the highly reactive metal species.

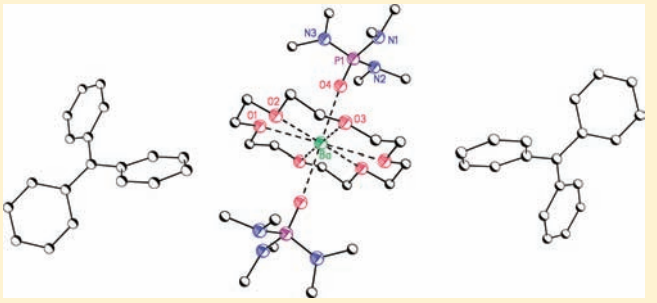

1. INTRODUCTION

The chemistries of the alkali (Li, Na, K, Rb, and Cs) and alkaline-earth metals (Be, Mg, Ca, Sr, and Ba) share similarities because of the filling of an s valence orbital. Because s-orbital electrons are easily released to form the respective mono- and dications, the metals are highly reactive toward oxygen and water, forming stable oxygen-containing compounds. Among these metals, lithium and magnesium have been the most intensely studied, rationalized by the importance of organolithium, Grignard, and diorganomagnesium reagents in synthetic applications.[1−3] In contrast, the exploration of heavy s-block metals has been set back by numerous synthetic challenges related to their (i) high oxo- and hydrophilicity, (ii) tendency toward cleaving ethers, (iii) large metal radii and resulting tendency toward aggregation and consequent solubility challenges, and (iv) largely electrostatic metal−ligand interactions, which result in significant lability and make the coordination chemistry of the metal strongly ligand- and coligand-dependent. s-Block metals represent the largest and most reactive metal families in the periodic table. Despite advances in the handling of these materials and available synthetic methodologies, limited research has been performed on the heavier congeners because of inherent synthetic challenges.

The benzylic and di- and triphenylmethanide anions were studied as early as 1900,[4,5] where the distinctly different colors of their solutions were noted. They can be regarded as derivatives of toluene, wherein one or two hydrogen atoms of the methyl substituent are replaced by phenyl rings. The anions are generated by deprotonation of a hydrogen atom in the benzyl carbon, or C_α, position. Triphenylmethane, $CHPh_3$, is the most acidic [pK_a = 30.6, dimethyl sulfoxide (DMSO)], followed by diphenylmethane, CH_2Ph_2 (pK_a = 32.2, DMSO), and finally, toluene, CH_3Ph, with pK_a = 41.0 (DMSO; Figure 1).[6,7] The respective

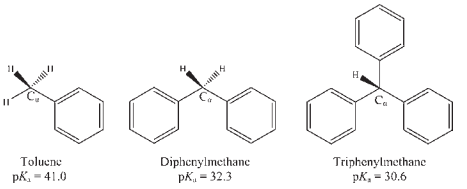

Figure 1. Benzyl-based ligands and relative pK_a values.[6,7]

ease of deprotonation may be rationalized by the ability of the ligand system to charge distribute with a direct influence on the stability of the resulting anions. Depending on the extent of the aromatic system, the anions display strong absorbance in the visible region, with a dark-orange color for $[CHPh_2]^-$ ($\lambda \sim 407-448$ nm) and a blood-red color for $[CPh_3]^-$ ($\lambda \sim 446-500$ nm).[8−12] s-Block benzylates, in addition to di- and triphenylmethanides, constitute a group of organometallics that nicely showcase patterns of reactivity and factors that affect the stability of the compounds, especially those pertaining to ion-association modes and the nature of the metal−ligand bond and including the ligand size and presence of noncovalent interactions.

The benzyl-based ligands can display several binding modes depending on both the nature of the metal center and the coligand present. Direct σ bonds between the metal and C_α are most prominent for smaller metals because more covalent interactions are preferred. However, with increasing of metal size, metal−π interactions become preferred, especially in the presence of sterically encumbered coligands.

Received: May 29, 2011
Published: September 29, 2011

Scheme 1. Ion-Association Modes for Alkali and Alkaline-Earth Metals

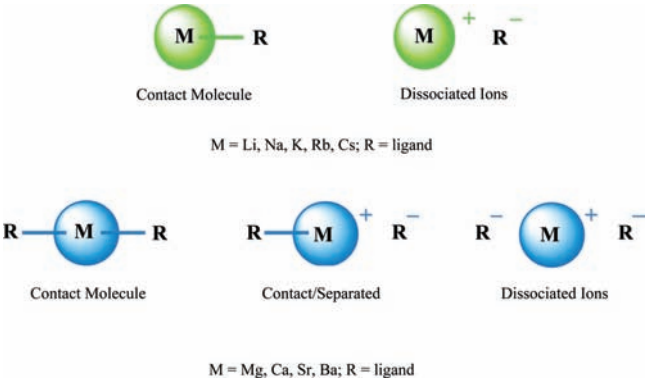

2. ION-ASSOCIATION MODES

The alkali and alkaline-earth metal benzylates and di- and triphenylmethanides (Figure 1) display a range of ion-association modes in both solution and the solid state (Scheme 1). Ranging from contact molecules, which involve direct σ bonds between the metal and organic ligand, to dissociated species observed when the cation is provided with effective coordinative saturation. In addition to the extent of charge distribution achieved by the ligands, many factors dictating the ion association of alkali and alkaline-earth metal derivatives apply to both groups of metals. These include (a) the nature of the metal−ligand bond, (b) the ligand size and the ability to distribute charge, and (c) the presence of secondary noncovalent interactions.

2.a. Metal−Ligand Bond. Metal−ligand bond characteristics are critically influenced by the metals' charge/size ratio. The lighter metals lithium, beryllium, and magnesium, with their smaller radii, display relatively high values; these decrease with increasing metal size. High charge/size ratios coincide with the capacity for bond polarization and the induction of bond covalency. As such, among the alkali and alkaline-earth metals, lithium, beryllium, and magnesium display metal−carbon bonds with the highest covalent character, leading to a preference for contact molecules.[13] For heavier congeners, differences in the electronegativities of the metal and ligand atoms coupled with an unfavorable overlap between the large metal centers and the small ligand orbitals, in addition to reduced charge/size ratios, result in predominantly ionic bonds and an increased tendency for ion dissociation.[1,3,14]

2.b. Ligand Size. Extensively documented, kinetic stabilization resulting from sterically demanding ligands has allowed the isolation of otherwise unstable compounds, including those with very low coordination numbers.[15−19] When descending the s-block metal groups, the radii of the metals significantly increase, making the heavy s-block metals the largest in the periodic table.[14] As a result, oligomerization is frequently observed, even in the presence of multidentate or sterically demanding ligands, negatively affecting the compound solubility and volatility.

2.c. Noncovalent Interactions. *2.c.1. Neutral Coligands.* In instances where the ligand bulk is not sufficient to provide adequate metal stabilization, coordination of neutral coligands has been effective in achieving steric saturation for large s-block metal centers to circumvent aggregation and increasing solubility. These coligands include monodentate oxygen-based Lewis bases such as diethyl ether (Et_2O), tetrahydrofuran (THF), and hexamethylphosphoramide (HMPA), in addition to multidentate ethers such as dimethoxyethane (DME), assorted multidentate glymes, or crown ethers. Additionally, nitrogen-based chelating donors such as the bidentate *N*,*N*,*N*′,*N*′-tetramethylethylenediamine (TMEDA) and the tridentate *N*,*N*,*N*′,*N*′,*N*″-pentamethyldiethylenetriamine (PMDTA) have been effective in isolating monomeric and stable s-block species. To this effect, studies delineating donor influences on compound stability and structure/function relationships have been instrumental in the further understanding of the coordination chemistry of these large metals.[3,20]

Ground-breaking work on the stabilization of alkali and alkaline-earth metals with crown ethers has led to a good understanding of the crown ether cavity size and metal diameter (Table 1). For alkali metals, variously sized crown ethers (12-crown-4, 15-crown-5, and 18-crown-6) have been successful in promoting ion dissociation.[17,21,22] For heavier alkaline-earth metals, ion dissociation can be achieved by the coordination of sterically encumbered neutral coligands often in combination with crown ethers. For example, strontium and barium may coordinate up to six HMPA coligands to form separated cations; also observed were combinations of two HMPA coligands with 18-crown-6.[23−29] Despite increased covalency, complete ion dissociation for magnesium compounds has been achieved through the use of 15-crown-5 in combination with THF and pyridine,[30,31] while the use of HMPA has afforded contact/separated species.[32] However, limited data are available on these systems.

2.c.2. Secondary Interactions. Despite the presence of neutral coligands, noncovalent interactions in the form of metal−π contacts are an important means to providing steric saturation of the large s-block metal centers. Although these are weaker than covalent interactions, they play a significant role in metal stabilization and ion association, especially because, frequently, multiple weak interactions add a cumulative effect. Typically arising from the resonance-stabilized anion, reported metal−π interactions fall below the sum of the van der Waals radii $[\Sigma(r_{wA} + r_{wC})]$ for a metal−carbon bond, and reported values for both alkali and alkaline-earth metals are summarized in Table 2.

3. SYNTHESIS

Because of the highly reactive nature of the s-block metals and resulting compounds, synthetic challenges have hampered the advancement of this chemistry. Notwithstanding, developments in the synthesis and handling of the highly reactive s-block benzylate and di- and triphenylmethanide compounds have provided a foundation for the further development of s-block organometallic chemistry. Reaction routes employed in the synthesis of target compounds are summarized in Scheme 2.

4. THE BENZYL LIGAND

Benzyllithium, CH_2PhLi, first introduced in the 1950s, was obtained by cleavage of benzyl ethers.[44] More convenient synthetic methods have since been developed, including metalation of toluene with alkyllithium (Scheme 2a, route i).[45] In the absence of a proper coligand, the lithium species display extended aggregation and poor solubility.

The role of neutral coligands on the compound stability and solubility has been aptly demonstrated by introducing various Lewis bases resulting in benzyllithium etherates of the type

Table 1. Alkali- and Alkaline-Earth-Metal Diameters and Crown Ether Cavity Diameters[a]

M^+/M^{2+}	CN	IR[14]	EN[33]	ionic diameter (Å)[34]	crown ether	cavity diameter (Å)	strongest binding
Li	6	0.76	0.97	1.20	12-crown-4	1.2−1.4	Li
Mg	6	0.72	1.23	1.30			
Na	6	1.00	1.04	1.98			
Ca	6	1.02	1.01	1.90	15-crown-5	1.7−2.2	Na, Mg
Sr	6	1.18	0.99	2.26			
K	6	1.35	0.89	2.66			
Ba	6	1.38	0.91	2.70	18-crown-6	2.6−3.2	Ca, Sr, Ba
Rb	6	1.52	0.89	2.96			K, Rb, Cs
Cs	6	1.67	0.86	3.34			

[a] CN = coordination number; IR = ionic radius; EN = electronegativity.

Table 2. van der Waals Radii and Metal−π Interaction Values for Alkali and Alkaline-Earth Metals

M^+/M^{2+}	CN	r_w[35] (C = 1.70) (Å)	$\Sigma(r_{wA} + r_{wC})$ (M−C) (Å)	experimental range[17,36−43] (Å)
Mg	6	1.73	3.43	2.25−2.79
Li	6	1.81	3.51	2.38−2.87
Ca	6	2.31	4.01	2.79−3.12
Na	6	2.27	3.97	2.86−3.08
Sr	6	2.49	4.19	2.98−3.38
Ba	6	2.68	4.38	3.07−3.48
K	6	2.75	4.45	2.78−3.57
Rb	6	3.03	4.73	3.20−3.64
Cs	6	3.43	5.13	3.25−3.97

$[Li(donor)_n(CH_2Ph)]_\infty$ [donor = THF (n = 2),[46] Et_2O (n = 1),[47] MeO^{t}Bu (n = 1);[48] Scheme 2a, routes i[46] and v[47]]. The etherates crystallize as polymeric chains, with alternating lithium and terminal dimethylbenzyl groups comprising the backbone (Figure 2). The benzyl rings in all three compounds adopt a planar arrangement, with only a slight average deviation of 12.5(4)° from the plane of the Li−C_α bond with the benzyl ring. Despite the presence of coligand and an increase in the overall coordinative metal saturation for the Et_2O species, a number of Li−C(π) interactions are observed (Table 3). Not surprisingly, additional THF coordination in $[Li(thf)_2(CH_2Ph)]_\infty$ leads to longer average Li−C bonds [THF = 2.335(1) Å; Et_2O = 2.212(8) Å; MeO^{t}Bu = 2.252(4) Å] consistent with an increase in the coordination number of the central lithium atom.

Demonstrating the importance of anion charge delocalization on the ion-association modes, the benzylic $[CH_2Ph]^-$ anion does not dissociate from the metals but rather displays contact molecules with σ bonds for alkali and alkaline-earth metals, even in the presence of multidentate neutral coligands. The reaction of alkyllithium with toluene in conjunction with triethylenediamine [$N(C_2H_4)_8N$; Scheme 2a, route i] also results in a polymeric chain $[Li(N(C_2H_4)_3N)(CH_2Ph)]_\infty$ but is propagated by the bidentate coligand coordinating to adjacent metal centers.[49] The closest Li−C(π) interaction is observed at the terminal C_α [2.21(2) Å], with two additional Li−C(π) interactions (Table 3).

For the larger potassium, the reaction of hexamethyldistannane with potassium metal in a THF/toluene mixture results in polymeric $\{(thf)[K(thf)(CH_2Ph)]_2\}_\infty$, which aggregates through multiple metal centers and is propagated by both intra- and intermolecular K−C(π) interactions from adjacent benzyl rings.[58] Coinciding with the increase in the metal size, from lithium to potassium (Table 1), the metal centers display coordination numbers ranging from 8 to 14.

The role of multidentate coligands is nicely demonstrated for a family of lithium benzylates in the presence of TMEDA, PMDTA, *N*,*N*′,*N*″-trimethyl-1,4,7-triazacyclononane (Me_3tacn), and *N*,*N*′,*N*″-trimethyl-1,4,7-triazacyclononane (Me_6tren) (Scheme 2a, route i), where monomeric species are observed.[50−53] In $Li(CH_2Ph)$(tmeda)(thf) (Figure 3), lithium displays a distorted tetrahedral geometry, with a Li−C_α bond of 2.210(5) Å.[51] Unexpectedly, a shorter Li−C bond length is observed for $Li(CH_2Ph)(Me_3tacn)$ [2.165(3) Å], where a distorted tetrahedral environment, due to the small bite angles from the coligand, is observed.[52] In both cases, one additional Li−C(π) interaction arises from the *ipso*-carbon, resulting in η^2 metal−ligand coordination (Table 3). Coordination to PMDTA in monomeric $Li(CH_2Ph)$(pmdta) allows for η^1 ligand coordination with a Li−C_α distance of 2.114(5) Å.[50] In the presence of Me_6tren, an increase in the coordination number of lithium results in an elongated Li−C_α bond of 2.344(3) Å.

The treatment of benzylpotassium with benzylmagnesium chloride in THF affords $Mg(CH_2Ph)_2(thf)_2$; however, structural information is not available for this species.[54] Displacement of coordinated THF was achieved by TMEDA, PMDTA, and *N*,*N*′-tetraethylethylenediamine (TEEDA), resulting in monomeric species of the type $Mg(CH_2Ph)_2$(donor). Mg−C and Mg−N distances were, on average, longer for the PMDTA adduct, as attributed to the higher metal coordination (Table 3). No additional M−C(π) interactions were reported, resulting in η^1 metal−ligand σ coordination for all three species.[54]

As a result of the increased metal size (Table 1), metalation of toluene with butylsodium in the presence of TMEDA (Scheme 2a, route i) allows for isolation of $[Na(tmeda)(CH_2Ph)]_4$, which crystallizes as a cyclic tetramer.[55] The coligand-stabilized sodium atoms form a nearly perfect square, with planar benzyl anions bridging the metal corners via Na−C_α interactions of 2.64 Å. A similar tetramer based on *o*-methylbenzyl (*o*-xylyl) is obtained in the presence of TMEDA, namely, $[Na(o\text{-xylyl})(tmeda)]_4$; however, poor crystal quality does not allow for further comparison.[56] Likewise, metalation of 1-ethylplhenyl in conjunction with TMEDA results in a polymeric species propagated by planar 1-ethylplhenyl anions, $[Na(tmeda)(1\text{-ethylphenyl})]_\infty$.[56] Na−$\eta^2$-C($\pi$) distances range from 2.691(1) to 2.866(1) Å. Despite the proven stabilization by sterically encumbering coligands for lithium and magnesium compounds, this principle is less effective for the larger metal centers, resulting in aggregation, as seen in the coordination

dx.doi.org/10.1021/ic201148d |*Inorg. Chem.* 2011, 50, 12223–12240

Scheme 2. Synthetic Routes toward s-Block Benzylates

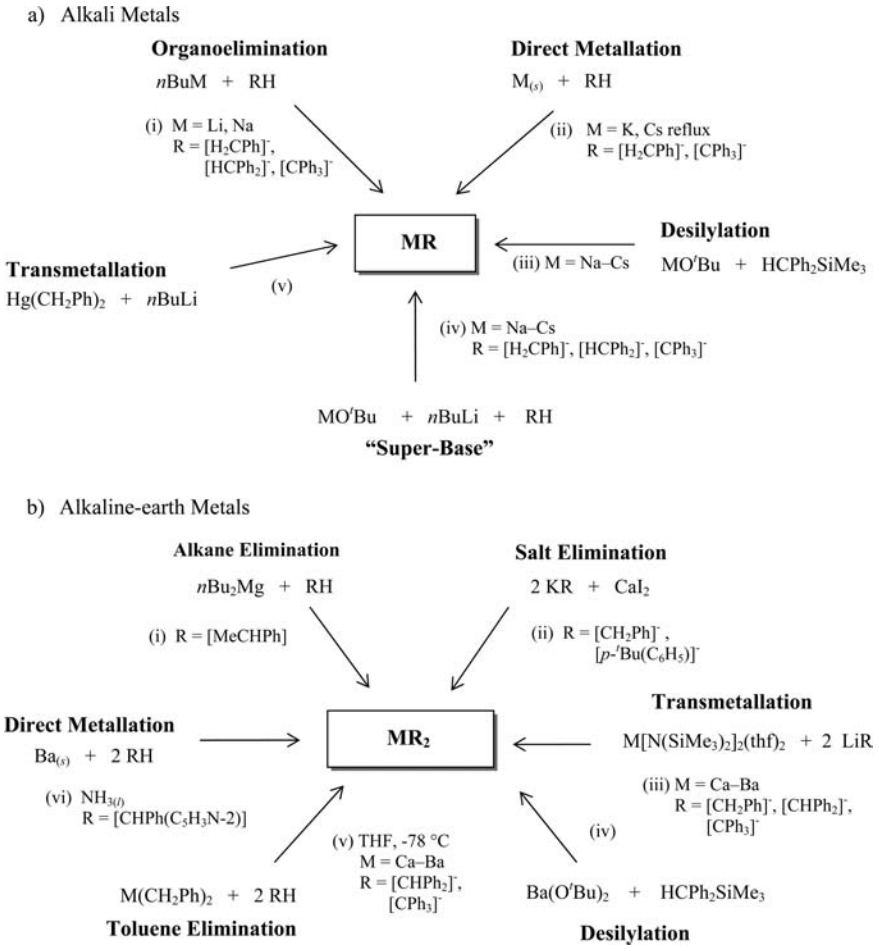

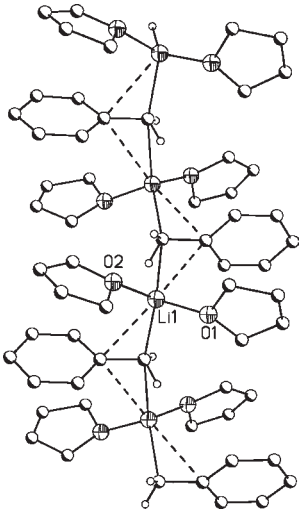

Figure 2. Crystal structure of $[Li(thf)_2(CH_2Ph)]_\infty$.[46] Li−C($\pi$) interactions are represented as dotted lines. Nonbenzylic hydrogen atoms are omitted for clarity.

polymers $[M(pmdta)(CH_2Ph)]_\infty$ (M = Na−Rb) (Scheme 2a, route iv), which also exhibit an increasing number of M−C(π) interactions with increasing metal radii (Table 3).[56,59]

While metalation of toluene via organosodium reagents afforded the sodium species,[56] the unavailability of stable heavy alkali-metal alkyl reagents necessitates the use of alternative reaction routes. For the heavier metal compounds, either potassium or rubidium *tert*-butoxides (K/RbO^{t}Bu) are combined in solution, with ^{n}BuLi creating "super-base" conditions and promoting deprotonation of toluene in nonpolar solvents (Scheme 2a, route iv).[59,60] While the sodium species does not exhibit M−C(π) interactions (η^1), the heavier metal compounds display an increasing degree of overall M−C(π) interactions of η^9 for potassium (Figure 4) and rubidium, despite coordination of PMDTA (Table 3). While each ligand exhibits η^3 intramolecular coordination to the metal center, the coordination polymers are propagated through η^6 intermolecular M−C(π) interactions from the benzylic anion bridging through adjacent metal centers.

Monomer formation for sodium and potassium has only been achieved in the presence of the multidentate Me$_6$tren, by adding the tetraamine to a toluene suspension of (CH$_2$Ph)M (M = Na, K).[53] Na(CH$_2$Ph)(Me$_6$tren) exhibits η^2 ligand coordination with a Na−C$_\alpha$ bond of 2.556(1) Å and a Na−C(π) interaction with a distance of 3.183(1) Å (Table 1). K(CH$_2$Ph)(Me$_6$tren) (Figure 5) does not exhibit a K−C$_\alpha$, but rather the metal prefers an η^6 ligand coordination mode, with K−C(π) interactions ranging from 3.097(3) to 3.0250(3) Å.

dx.doi.org/10.1021/ic201148d |*Inorg. Chem.* 2011, 50, 12223–12240

Table 3. Selected Bond Lengths for s-Block Benzylates

	CN	hapticity of the ligand	M−C_α (Å)	M−donor (Å)[a]	M−C(π) (Å)	ref
$[Li(Et_2O)(CH_2Ph)]_\infty$	5	μ−η^2:η^2	2.212(8)	1.948(8)	2.404(9)−2.865(9)	47
$[Li(MeO^tBu)(CH_2Ph)]_\infty$	5	μ−η^2:η^2	2.252(4)	1.925(4)	2.384(4)−2.544(4)	48
$[Li(thf)_2(CH_2Ph)]_\infty$	6	μ−η^2:η^2	2.335(1)	1.981(1)	2.823(1)	46
$[Li(triethylenediamine)(CH_2Ph)]_\infty$	5	η^3	2.21(2)	2.10(1)	2.39(2)−2.58(2)	49
$[Li(Me_2N(CH_2)_2OMe)(CH_2Ph)]_4$	4	μ−η^1:η^1	2.306(2)	2.033(2)[a]		50
				2.138(2)[b]		
$Li(CH_2Ph)(tmeda)(thf)$	5	η^2	2.210(5)	1.973(5)[a]	2.722(5)	51
				2.148(5)[b]		
$Li(CH_2Ph)(pmdta)$	4	η^1	2.114(5)	2.125(5)		50
$Li(CH_2Ph)(Me_3tacn)$	5	η^2	2.165(3)	2.148(5)	2.731(2)	52
$Li(CH_2Ph)(Me_6tren)$	5	η^1	2.344(3)	2.247(3)		53
$Mg(CH_2Ph)_2(tmeda)$	4	η^1	2.170(2)	2.199(2)		54
$Mg(CH_2Ph)_2(teeda)$	4	η^1	2.178(2)	2.196(2)		54
$Mg(CH_2Ph)_2(pmdta)$	5	η^1	2.229(1)	2.338(1)		54
$[Na(tmeda)(CH_2Ph)]_4$	4	μ−η^1:η^1	2.64	2.50		55
$[Na(pmdta)(CH_2Ph)]_\infty$	5	μ−η^1:η^1	2.770(10)	2.584(8)		56
$Na(CH_2Ph)(Me_6tren)$	6	η^2	2.556(1)	2.496(1)	3.183(1)	53
$[Na(tmeda)(1\text{-ethylphenyl})]_\infty$	5	μ−η^2:η^1	2.691(1)	2.528(2)	2.691(1)−2.866(1)	56
$Ca(CH_2Ph)_2(thf)_4$	6	η^1	2.581(6)	2.397(3)		57
$Ca[(p\text{-}^tBu)CH_2Ph]_2(thf)_4$	6	η^1	2.597(2)	2.388(2)		57
$\{(thf)[K(thf)(CH_2Ph)]_2\}_\infty$	8−14	μ^4-η^6:η^3:η^2:η^1	3.005	2.73	3.050−3.421	58
$[K(pmdta)(CH_2Ph)]_\infty$	12	μ−η^6:η^3	3.171(2)	2.915(2)	3.150(2)−3.297(2)	59
$K(CH_2Ph)(Me_6tren)$	10	η^6		2.849(3)	3.097(3)−3.0250(3)	53
$[Rb(pmdta)(CH_2Ph)]_\infty$	12	μ−η^6:η^3	3.270(2)	3.036(1)	3.141(2)−3.569(2)	59

[a] a = oxygen-based donor; b = nitrogen-based donor.

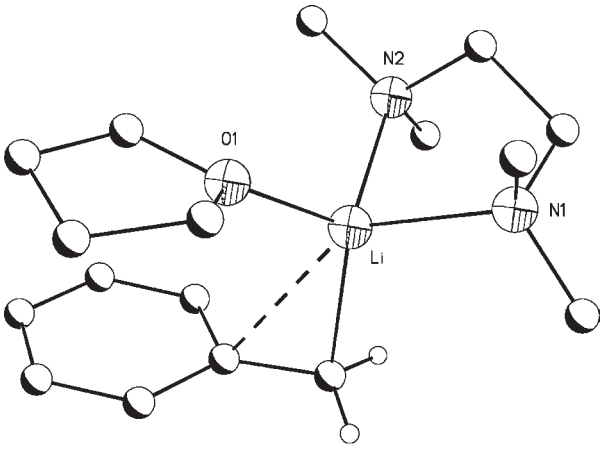

Figure 3. Crystal structure of $Li(CH_2Ph)(tmeda)(thf)$.[51] Li−C(π) interactions are represented as dotted lines. Nonbenzylic hydrogen atoms are omitted for clarity.

Regardless of many similarities in the handling and preparation of alkali and alkaline-earth organometallic species, examples of heavy alkaline-earth-metal benzyl derivatives remain scarce. Salt metathesis reactions (Scheme 2b, route ii) between the readily synthesized benzylpotassium species and CaI_2 afford the stable benzylcalcium complexes $Ca(R)_2(thf)_4$ [R = CH_2Ph, $(p\text{-}^tBu)CH_2Ph$].[57] Both crystallize in slightly distorted octahedral environments, however, $Ca(CH_2Ph)_2(thf)_4$ displays a cis geometry, while $Ca[(p\text{-}^tBu)CH_2Ph]_2(thf)_4$ adopts a trans geometry, as attributed to crystal packing effects (Figure 6).

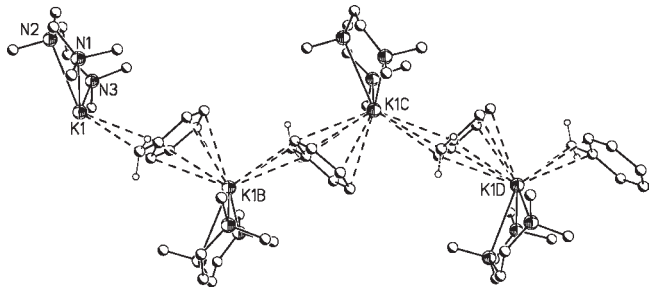

Figure 4. Crystal structure of $[K(pmdta)(CH_2Ph)]_\infty$.[59] K−C($\pi$) interactions are represented as dotted lines. Nonbenzylic hydrogen atoms are omitted for clarity.

Structural information on the strontium and barium analogues is unknown because of high reactivity and poor solubility. Upon realization of the importance of the compounds as powerful starting materials for a variety of alkaline-earth-metal derivatives, recent efforts have focused on making these compounds more accessible. Benzyl derivatives have been successfully used to prepare families of di- and triphenylmethanides,[3,61−65] acetylides,[66] and amides.[67] However, inherent setbacks resulting from high reactivity in ether and insolubility of the benzyl derivatives in hydrocarbons pose limitations to the route. Ether scission reactions in THF solutions may be suppressed by utilizing low temperatures (−78 °C).[3]

Synthetic access to the reagents is also provided by redox transmetalation involving the reaction of a barium mirror with dibenzylmercury.[57,68−72] A more convenient route involves

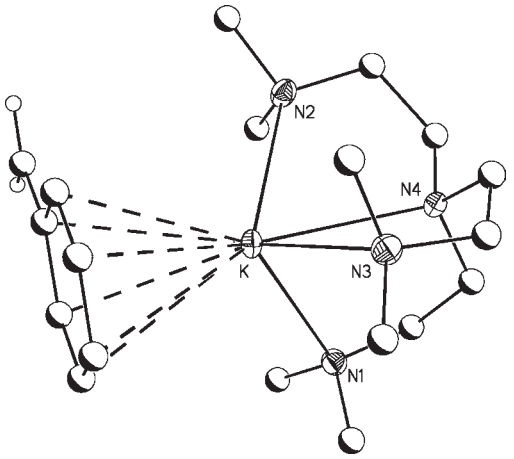

Figure 5. Crystal structure of $K(CH_2Ph)(Me_6tren)$.[53] K−C(π) interactions are represented as dotted lines. Nonbenzylic hydrogen atoms are omitted for clarity.

reaction of the easily accessible $Ba[N(SiMe_3)_2]_2(thf)_2$ with the transmetalation reagent $Li(CH_2Ph)$tmeda in Et_2O (Scheme 2b, route iii).[73] This results in the clean precipitation of the dibenzylbarium species. A variation of this scheme provides access to the strontium congener in high yields and purity.[61] Similar chemistry for the calcium analogue has been difficult, as shown recently with isolation of the heterometallic benzyl calciate obtained by the treatment of benzyllithium with $Ca[N(SiMe_3)_2]_2(thf)_2$ in the presence of TMEDA (Figure 7). The calciate can also be obtained by the treatment of $Ca(CH_2Ph)_2(thf)_4$ with 2 equiv of $Li(CH_2Ph)$tmeda (eq 1).[74] A comparison of the reactivity between the homometallic $Ca(CH_2Ph)_2(thf)_4$ and the calciate shows significantly increased reactivity for the heterobimetallic calciate species, a result in agreement with the reactivity trends of other alkaline-earth organometallic "ate" complexes.[39,75−93]

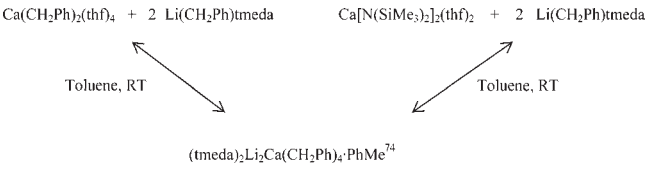

The calciate exhibits a linear array of three metal centers with a central calcium atom framed by two lithium atoms. The metal centers are bridged by benzyl moieties with Ca−C_α [2.610(5) Å] and Li−C_α distances [2.283(7) Å]. Not surprisingly, these are longer than those in homometallic $Ca(CH_2Ph)_2(thf)_4$ [Ca−C_α = 2.2568(5)−2.595(5) Å][57] and $Li(CH_2Ph)(tmeda)(thf)$ [Li−C_α = 2.210(5) Å],[51] likely a consequence of the bridging nature of C_α (Table 3). The coordination sphere of the larger calcium is supplemented by several secondary interactions, including a Ca−C(π) interaction to the *ipso*-carbon [2.972(5) Å] resulting in η^2-benzyl coordination, in addition to a M···H−C agostic interaction involving a benzylic hydrogen atom (2.33 Å; Table 4).[67]

Metalation of toluene with a mixture of ^{n}BuLi/^{n}BuNa in the presence of excess TMEDA resulted in the formation of a mixed alkali-metal benzyl cyclic tetramer, $(tmeda)_4Li_2Na_2(CH_2Ph)_4$.[94] The coligand-stabilized lithium and sodium atoms form a nearly perfect square, with alternating metal vertices. Planar benzyl

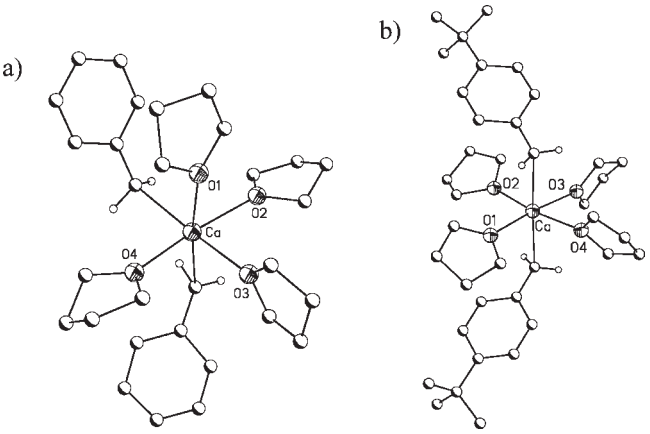

Figure 6. (a) Crystal structure of $Ca(CH_2Ph)_2(thf)_4$ displaying cis geometry. (b) Crystal structure of $Ca[(p\text{-}^tBu)CH_2Ph]_2(thf)_4$ displaying trans geometry.[57] Nonbenzylic hydrogen atoms are omitted for clarity.

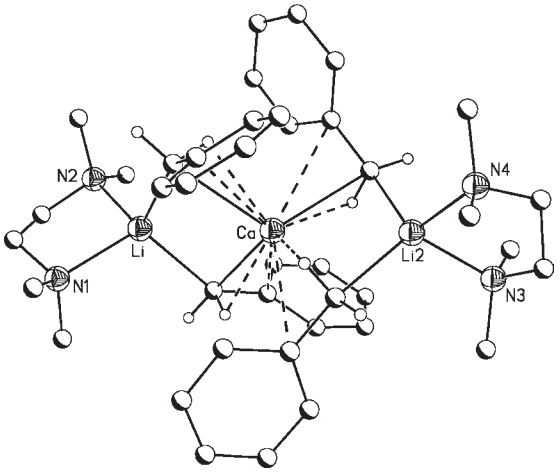

Figure 7. Crystal structure of $(tmeda)_2Li_2Ca(CH_2Ph)_4$.[74] Ca−C($\pi$) and Ca···H−C agostic interactions are represented as dotted lines. Nonbenzylic hydrogen atoms are omitted for clarity.

anions bridge the metal edges via M−η^2-C(π) interactions ranging from 2.742(6) to 2.853(5) Å (Table 4), similar to $[Na(tmeda)(CH_2Ph)]_4$.[55]

Heterometallic formation is also observed for magnesium with isolation of the benzyl magnesiate $[Li(tmeda)_2][(CH_2Ph)\text{-}Mg(\mu\text{-}CHPh)_2Li(tmeda)]$,[93] obtained by the reaction of ethyllithium and diethylmagnesium in the presence of excess TMEDA in toluene. Two TMEDA molecules fully saturate the lithium atom, promoting separation of one of the lithium ions. The anion is comprised of a four-coordinate magnesium metal center coordinated to two bridging benzyl ligands and two terminal η^1-coordinate benzyl ligands. The lithium center in the anion is also four-coordinate, with η^1 metal−ligand coordination. Further stabilization is provided by a TMEDA coligand. The Mg−C_α distances are, on average, longer for the bridging C_α [2.319(9) Å] than for the terminal benzyl carbon [2.225(11) Å], consistent with the higher coordination on C_α.

Metalation of 2,2′,6,6′-tetramethyl-1,1′-biphenyl, $(2\text{-}CH_2\text{-}6\text{-}(CH_3)(C_6H_3)_2\text{-}2',6'\text{-}(CH_3)_2)$, in the presence of PMDTA results in the monomeric η^1 species $Li(2\text{-}CH_2\text{-}6\text{-}(CH_3)\text{-}(C_6H_3)_2\text{-}2',6'\text{-}(CH_3)_2)(pmdta)$.[95] In the presence of a large

Table 4. Selected Bond Lengths for Heterobimetallic s-Block Benzylates

	CN[a]	hapticity of the ligand	M−C_α (Å)[a]	M−donor (Å)[a]	M−C(π) (Å)[a]	ref
$(tmeda)_4Li_2Na_2(CH_2Ph)_4$	6[a,b]	$\mu-\eta^2:\eta^2$	2.399(6)[a]	2.321(6)[a]	2.742(6)−2.853(5)	94
			2.529(6)[b]	2.421(6)[b]		
$[Li(tmeda)_2]$ $[(CH_2Ph)Mg(\mu\text{-}CHPh)_2Li(tmeda)]$	4[x]	$\mu-\eta^1:\eta^{1a}$	2.281(10)[y,c]	2.135(22)[x]		93
	4[y,a,c]	η^{1c}	2.225(18)[y,a]	2.138(21)[y,a]		
$(tmeda)_2Li_2Ca(CH_2Ph)_4$	11[d]	$\mu-\eta^2:\eta^1$	2.610(5)[d]	2.109(5)[a]	2.972(5)[d]	74
	4[a]		2.283(7)[a]			

[a] a = Li; b = Na; c = Mg; d = Ca; x = cation; y = anion.

Table 5. Selected Bond Lengths for s-Block-Substituted Benzylates

	CN[a]	hapticity of the ligand	M−C_α (Å)[a]	M−donor (Å)[a]	M−C(π) (Å)[a]	ref
$Li(2\text{-}CH_2\text{-}6\text{-}(CH_3)(C_6H_3)_2\text{-}2',6'\text{-}(CH_3)_2)(pmdta)$	4	η^1	2.141(2)	2.126(7)		95
$[Li(tmeda)_2][(tmeda)Li(CH_2C_6H_3\text{-}3,5\text{-}Me_2)_2]$	4[a]	η^2	2.291(7)[b]	2.121(6)[a]	2.637(6)[b]	96
	4[b]			2.165(6)[b]		

[a] a = cation; b = anion.

excess of TMEDA, metalation of mesitylene, (2,4,6-trimethylbenzene) (Scheme 2a, route i), results in the formation of the separated ion pairs $[Li(tmeda)_2][(tmeda)Li(3,5\text{-}(CH_3)_2\text{-}CH_2C_6H_3)_2]$.[96] The lithiate anion is comprised of a four-coordinate lithium metal center bound to two η^1-coordinate benzyl groups and the bidentate TMEDA. Because of a slight increase in the ligand bulk for mesitylene compared to the benzyl anion, the Li−C_α bond lengths are slightly longer, 2.257(7) and 2.325(7) Å, than average for reported benzyllithiums, 2.212 Å (Table 5). Only one Li−C(π) interaction is observed between the metal center and the *ipso*-carbon of the tighter bound ligand [2.637(6) Å], resulting in η^2 hapticity.

Aside from their propensity as polymerization initiators,[97−101] benzyl-based alkaline-earth-metal compounds are ideally suited as starting materials for a variety of heavy alkaline-earth organometallics,[3,61−67] with limitation to ligands with a lower pK_a than toluene (41, DMSO)[6,7] and its derivatives (Scheme 2a, route v). However, because of the high reactivity of the benzyl derivative, especially in the presence of ethereal solvents, reaction conditions need to be carefully chosen. The sensitivity toward ethers is a significant limitation because of the limited solubility of the benzyl derivatives in hydrocarbons.[102] As such, the use of THF at −78 °C has been effective.

5. DIPHENYLMETHANE LIGAND

While extensive work exists for benzyl derivatives, significantly less is known on the diphenylmethanide counterparts. Setbacks include high reactivity, low solubility, and limited availability of suitable starting materials, but recent advances have afforded families of compounds that aid in the improved understanding of the factors affecting metal stabilization.

Diphenylmethane can be regarded as a derivative of toluene, where one hydrogen atom on the benzylic carbon is replaced by a phenyl ring (Figure 1). This change results in increased steric demand and capacity for charge delocalization. The more effective charge distribution renders ion dissociation more prevalent, especially in the presence of multidentate coligands. Analogous attempts to prepare a separated benzyl anion have been unsuccessful because of ether scission in THF. The following examples will illustrate recent advances in synthetic protocol,

Scheme 3. Representations of the Two "Flip" Orientations of Diphenylmethanide

I II

the impact of the nature of neutral coligands, and overall structure−reactivity functions.

The diphenylmethanide anion can frequently display a "flip" conformational disorder (Scheme 3), which may or may not involve a center of symmetry.[61,64,103] Surprisingly, this disorder can be observed in both separated and contact species, providing a rationale on the scarcity of solid-state data.

For the smaller metals lithium and sodium, availability of the metallating agents ^{n}BuLi and ^{n}BuNa allows the straightforward synthesis of diphenylmethanide species. The reaction of ^{n}BuLi and diphenylmethane in the presence of 12-crown-4 affords the dissociated ion pair $[Li(12\text{-crown-}4)_2][CHPh_2]$ (Figure 8).[104] Despite the expected prevalence for σ bonding, the addition of a crown ether provides effective steric saturation of the metal center. The $[CHPh_2]^-$ anion effectively distributes the negative charge, as expressed through a planar central carbon atom and coplanarity of the phenyl rings with a wide $C_\alpha-C_i-C_\alpha$ angle of 132.1(4)°, features that are also common in the anions of other alkali-metal diphenylmethanides. Therefore, only deviations in these values will be addressed.

Exhibiting the reactive nature and instability of diphenylmethanide complexes, reactions of ^{n}BuLi, diphenylmethane, and PDMTA in THF at room temperature resulted in novel lithium enolate complex $[Li_2(OCHCH_2)(pmdta)_2][CHPh_2]$,[64] likely the result of ether cleavage reactions. THF is known to decompose into ethylene and enolate after deprotonation.[1,102,105] The compound crystallizes as a dissociated ion pair with a bimetallic lithium cation, where the four-coordinate metal centers are bridged by an enolate $(OCHCH_2)^-$ fragment. Further metal coordination is provided by terminal PMDTA coligands (Figure 9). Additional Li−C(π) interactions arising from the

dx.doi.org/10.1021/ic201148d |*Inorg. Chem.* 2011, 50, 12223–12240

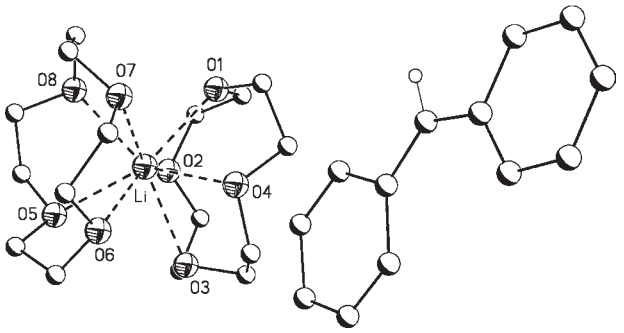

Figure 8. Crystal structure of $[Li(12\text{-crown-}4)_2][CHPh_2]$.[104] Nonbenzylic hydrogen atoms are omitted for clarity.

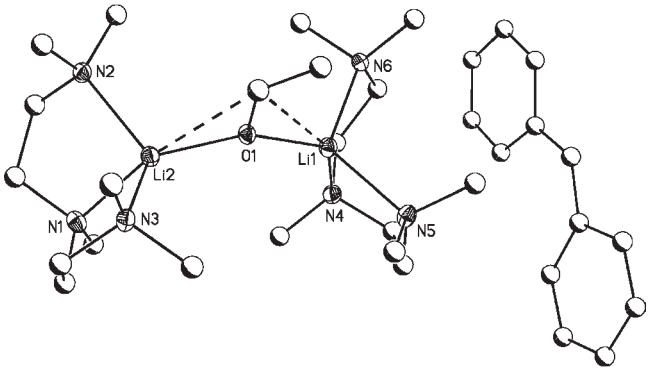

Figure 9. Crystal structure of $[Li_2(OCHCH_2)(pmdta)_2][CHPh_2]$.[64] Li−C($\pi$) interactions are represented as dotted lines. Hydrogen atoms are omitted for clarity.

C═C bond are observed with distances of 2.542(3) and 2.662(3) Å for each lithium atom.

The tetrameric species $[Na(tmeda)(CHPh_2)]_4$ (Figure 10) is obtained by the treatment of diphenylmethane with butylsodium in the presence of TMEDA (Scheme 2a, route i).[56] Each $[CHPh_2]^-$ anion bridges two metal centers through η^2 coordination; however, different regions of the ligand are involved in these contacts. On the one side, the metal center coordinates to C_α and the *ipso*-carbon from one of the phenyl groups with distances of 2.661(8)−2.858(8) Å (Table 6). Intermolecular η^2 coordination is also observed through Na−C(π) interactions from the phenyl group of a neighboring anion [2.956(1) and 2.962(1) Å]. Replacing TMEDA with PMDTA results in isolation of the monomeric species $Na(CHPh_2)(pmdta)$, with Na−η^5-C(π) interactions ranging from 2.628(4) to 3.018(4) Å.[56] The combination of the larger PMDTA coligand and the more sterically encumbering diphenylmethanide anion allows for better stabilization of the metal center, circumventing aggregation.

However, the larger sized diphenylmethanide anion alone compared to benzyl is not capable of reducing aggregation for the heavier alkali metals. Reactions of ^{n}BuLi with KO^{t}Bu in the presence of THF afforded the polymeric $[K(CHPh_2)(thf)_{0.5}]_\infty$.[106] Two metal centers are coordinated to the same THF molecule; each metal center is also directly bonded to C_α [3.003(5) Å]. Further metal coordination is provided by several K−C(π) interactions ranging from 3.067(3) to 3.566(5) Å to the phenyl groups of the ligand coordinated to the adjacent metal center (Table 6). The polymer is propagated by further intermolecular K−C(π) interactions to neighboring units.

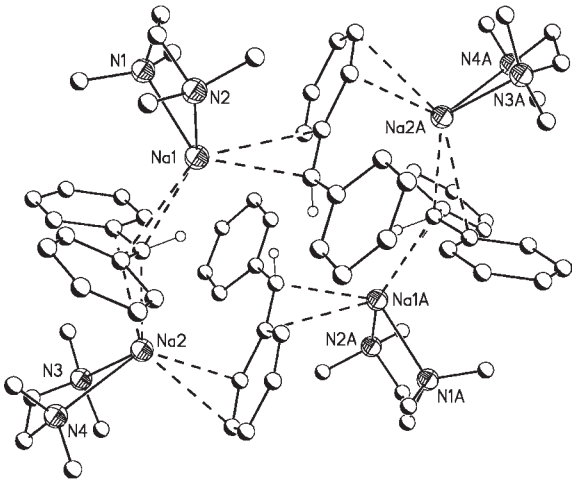

Figure 10. Crystal structure of $[Na(tmeda)(CHPh_2)]_4$.[56] Na−C(π) interactions are represented as dotted lines. Nonbenzylic hydrogen atoms are omitted for clarity.

Similar to the ease of preparation of lithium and sodium benzylate complexes, the availability of alkyllithium and alkylsodium reagents affords stable diphenylmethanide species. However, increased reactivity of the heavier alkali metals and impediments concerning the preparation of alkali organometallics have hampered isolation of comparable heavy alkali-metal species. "Super-base" conditions, used extensively for the corresponding benzylates (Scheme 2a, route iv),[60] are troublesome for diphenylmethanides because of difficulties in separating the target compounds from the lithium alkoxide side product. Other impediments include the lack of selective metalation and potential ether scission chemistry.[103,107]

An alternative reaction route, based on prior chemistry with phosphides and silanides,[108−110] involves the use of a $-SiMe_3$-substituted diphenylmethane in conjunction with alkali *tert*-butoxides, resulting in a desilylation pathway to obtain clean alkali diphenylmethanides (Scheme 2a, route iii).[103] Although lithium $-SiMe_3$-substituted diphenylmethanides have been reported via direct metalation reactions under retention of $-SiMe_3$,[111] the greater ionic nature of the heavier metal alkoxides promotes $-SiMe_3$ cleavage under the formation of silyl ether. The target compounds are prepared in hydrocarbon solvents under ambient reaction conditions in the presence of appropriately sized crown ethers.

The desilylation synthetic pathway (Scheme 2a, route iii) proved to be a powerful preparation method for a family of heavy alkali-metal diphenylmethanides, described below.[103,112] In a typical reaction, the addition of crown ether was necessary to suppress aggregation. The size of the crown ether has a direct impact on the coordinative metal saturation and overall stability of the resulting compounds. The use of 12-crown-4 in conjunction with rubidium resulted in a dissociated ion pair, $[Rb(12\text{-crown-}4)_2][CHPh_2]$,[103] where two of the small crown ethers (1.2−1.4 Å) arrange in a sandwich-type fashion to fully saturate the metal center similar to $[Li(12\text{-crown-}4)_2][CHPh_2]$.[104] Likewise, coordination of 15-crown-5 (1.7−2.2 Å) for potassium (2.66 Å) or rubidium (2.96 Å) $[M(15\text{-crown-}5)_2][CHPh_2]$ (M = K, Rb) affords sandwich-type metal coordination.[103] The separated $[CHPh_2]^-$ anion is found to be planar in these instances and does not display any close contacts with the metal centers.

Table 6. Selected Bond Lengths for Alkali-Metal Diphenylmethanides

	CN	hapticity of the ligand	M−C_α (Å)[a]	M−donor (Å)[a]	M−C(π) (Å)	ref
$[Li_2(OCHCH_2)_2(pmdta)_2][CHPh_2]$	5			1.904(3)[a]	2.542(3)−2.662(3)	64
				2.138(3)[b]		
$[Li(12\text{-crown-}4)_2][CHPh_2]$	8			2.366(2)		104
$[Na(tmeda)(CHPh_2)]_4$	6	$\mu-\eta^2:\eta^2$	2.661(8)	2.497(2)	2.721(8)−2.962(1)	56
$Na(CHPh_2)(pmdta)$	8	η^5	2.628(4)	2.454(4)	2.756(5)−3.018(4)	56
$[K(CHPh_2)(thf)_{0.5}]_\infty$	11	$\mu-\eta^6:\eta^3$	3.003(5)	2.778(4)	3.067(3)−3.566(5)	106
$[K(15\text{-crown-}5)_2][CHPh_2]$	10			2.896(5)		103
$[K(18\text{-crown-}6)(thf)_2][CHPh_2]$	8			2.702(4)[c]		103
				2.802(4)[d]		
[K(2,2,2)cryptand][$CHPh_2$]	8			3.0199(5)[e]		103
				2.8209(5)[f]		
$[Rb(12\text{-crown-}4)_2][CHPh_2]$	8			2.918(4)		103
$[Rb(15\text{-crown-}5)_2][CHPh_2]$	10			2.995(4)		103
$Rb(CHPh_2)(18\text{-c-}6)$	9	η^3	3.063(3)	2.932(5)	3.311(3)−3.393(3)	112
$Rb(CHPh_2)(18\text{-crown-}6)(thf)$	13	η^6		3.143(5)[c]	3.250(3)−3.491(3)	112
				2.850(5)[d]		
[Rb[2.2.2]cryptand][$CHPh_2$]	8			3.022(1)[e]		103
				2.868(9)[f]		
$[Cs_2(18\text{-crown-}6)_3][CHPh_2]_2$	12			3.481(4)		103
$Cs(CHPh_2)([2.2.2]cryptand)$	13	η^5	3.302(8)	3.124(4)[e]	3.473(5)−3.685(8)	103
				3.219(4)[f]		

[a] a = enolate; b = PMDTA; c = THF; d = 18-crown-6; e = nitrogen; f = oxygen.

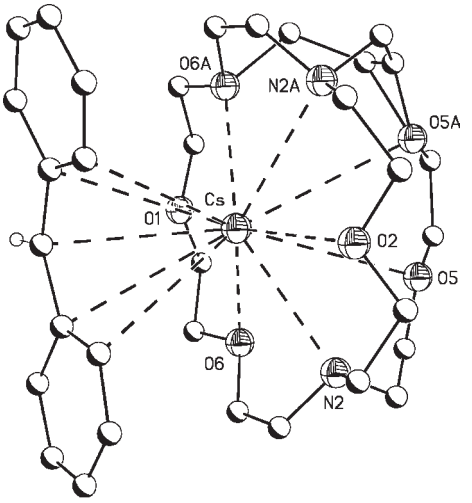

Figure 11. Crystal structure of $Cs(CHPh_2)([2.2.2]cryptand)$.[103] Cs−C($\pi$) interactions are represented as dotted lines. Nonbenzylic hydrogen atoms are omitted for clarity.

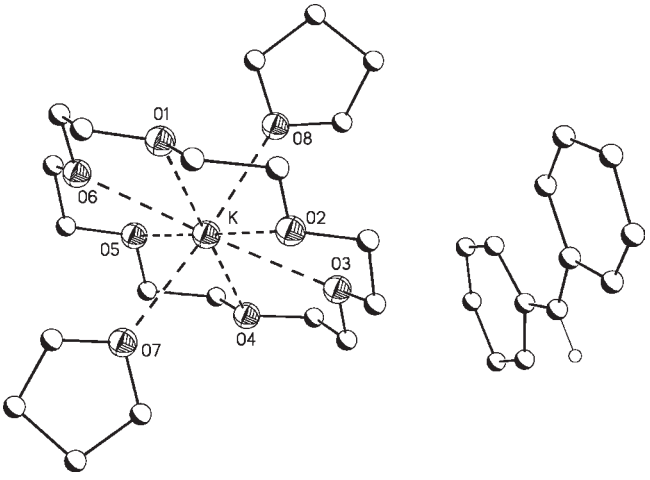

Figure 12. Crystal structure of $[K(18\text{-crown-}6)(thf)_2][CHPh_2]$.[103] Nonbenzylic hydrogen atoms are omitted for clarity.

The use of the larger, three-dimensional [2.2.2]cryptand also affects the charge separation for the rubidium and potassium analogues under the formation of [M([2.2.2]cryptand)][$CHPh_2$] (M = K, Rb).[103] Again, the $[CHPh_2]^-$ anion is found to be planar; no close contacts with the metal centers are observed. However, the steric saturation provided by the cryptand is not sufficient to fully encapsulate a cesium metal center (3.34 Å), resulting in the formation of a contact molecule involving an η^5-coordinate $[CHPh_2]^-$ anion in $Cs(CHPh_2)([2.2.2]cryptand)$ (Figure 11).[103] This molecule exhibits a Cs−C_α contact of 3.302(8) Å, with additional Cs−C(π) interactions ranging from 3.473(5) to 3.685(8) Å (Table 6).

While sandwiched-type metal cations were isolated in the presence of 12-crown-4 and 15-crown-5, the use of 18-crown-6 (2.6−3.2 Å) in conjunction with potassium afforded the separated ion pair $[K(18\text{-crown-}6)(thf)_2][CHPh_2]$ with the metal center located in the plane of the crown ether, while two THF coligands occupy the axial positions (Figure 12).[103] Showcasing that the prediction of the molecular geometry is not straightforward, the rubidium analogue displays two distinctly different metal−ligand geometries, depending on the respective temperatures of crystallization.[112] Crystal growth at −23 °C resulted in the η^3 contact molecule $Rb(CHPh_2)(18\text{-crown-}6)$ (Figure 13a), with the metal located slightly above the plane of the crown ether and the exposed metal face capped by the ligand and two

dx.doi.org/10.1021/ic201148d |Inorg. Chem. 2011, 50, 12223–12240

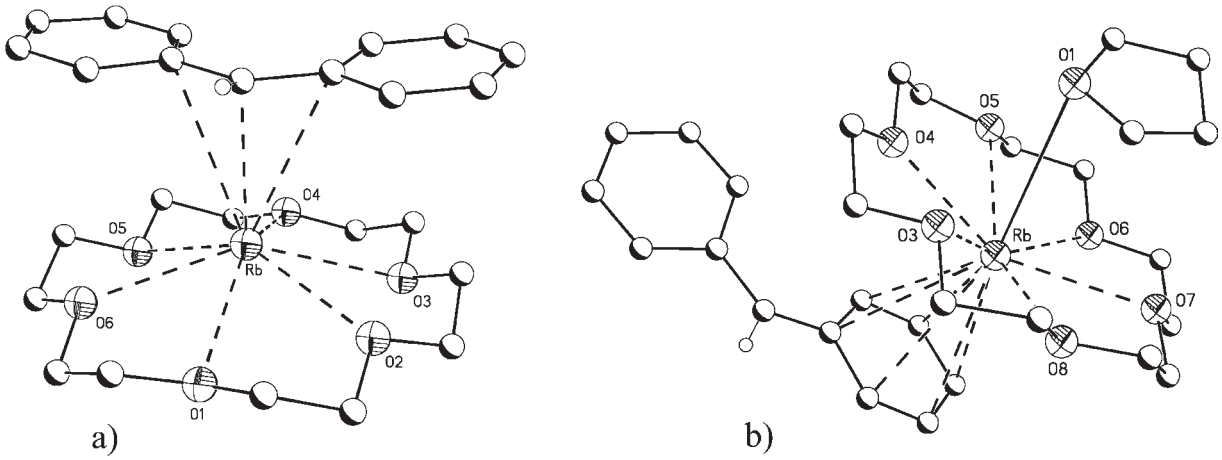

Figure 13. (a) Crystal structures of $Rb(CHPh_2)$(18-crown-6) (b) and $Rb(CHPh_2)$(18-crown-6)(thf).[112] Rb−C(π) interactions are represented as dotted lines. Nonbenzylic hydrogen atoms are omitted for clarity.

additional Rb−C(π) interactions arising from the *ipso*-carbon atoms of the phenyl groups [3.311(3)−3.393(3) Å; Table 6]. In this case, the Rb−C_α distance is 3.063(3) Å. Crystallization at 4 °C results in the formation of an η^6-coordinated rubidium diphenylmethanide, $Rb(CHPh_2)$(18-crown-6)(thf) (Figure 13b).[112] Again, the metal lies slightly above the plane of the crown ether, while one of the exposed metal faces is capped by a THF molecule and the other saturated by six Rb−C(π) interactions [3.250(3)−3.491(3) Å] from one of the phenyl groups of the ligand.

In the case of cesium, sandwich-type metal coordination is effective, as shown with the separated ion species, $[Cs_2(18\text{-crown-}6)_3][CHPh_2]_2$, where no additional Cs−C(π) interactions with $[CHPh_2]^-$ are observed.[103] The anions display resonance-stabilized, planar geometries with $C_i-C_\alpha-C_i$ angles in the range of 131−133°, consistent with previously discussed diphenylmethanides.[56,64,104] In all cases, the anion demonstrates the expected resonance stabilization, although a slight elongation of the C_i-C_o bonds in line with other separated $[CHPh_2]^-$ is observed.[56,104]

The development of the desilylation pathway for alkali-metal diphenylmethanides proved to be instrumental in the preparation of some of the above complexes. However, synthetic challenges in preparing the corresponding *tert*-butoxides for the heavy alkaline-earth metals prevented analogous chemistry. Notably, the majority of diphenylmethanide compounds are based on the larger alkaline-earth metal barium, likely because of the availability of dibenzylbarium as an effective starting material.

In an extension of the desilylation route (Scheme 2b, route iv), a single example using in situ prepared barium *tert*-butoxide afforded both the contact molecule $Ba(CHPh_2)_2$(18-crown-6) (Figure 14) and the ether cleavage product $[\{Ba(18\text{-crown-}6)(OC_2H_3)(thf)\}_2][CHPh_2]_2$ (Figure 15).[61] Curiously, in contrast to the alkali desilylation pathway, the addition of ^{n}BuLi was necessary for product formation. In the σ-bonded $Ba(CHPh_2)_2$-(18-crown-6) species, the metal center is in a pseudooctahedral environment, with the crown ether occupying the equatorial plane. Despite the presence of THF, the ligands coordinate to the metal center at the axial positions, with an average Ba−C_α bond length of 3.081(3) Å (Table 7). Only one additional Ba−C(π) interaction is observed from the *ipso*-carbon of one of the phenyl rings with a length of 3.389(3) Å. As a consequence of this

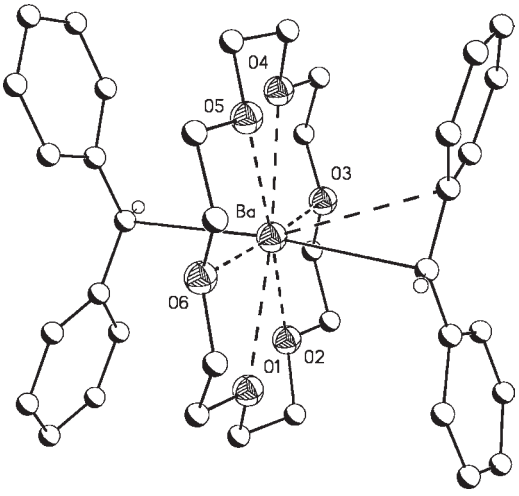

Figure 14. Crystal structure of $Ba(CHPh_2)_2$(18-crown-6).[61] Nonbenzylic hydrogen atoms are omitted for clarity.

interaction, the $C_i-C_\alpha-C_i$ angles for both ligands are slightly smaller, 127.9(4)° and 129.2(4)°, than those observed for the alkali congeners (131−133°).

While $Ba(CHPh_2)_2$(18-crown-6) displays a Ba−C σ bond, the barium enolate $[\{Ba(18\text{-crown-}6)(OC_2H_3)(thf)\}_2][CHPh_2]_2$ adopts a doubly enolate-bridged barium diphenylmethanide dimer. The crown ethers are tipped toward each other, allowing interaction with the enolate moieties, while the barium centers lie above the plane of the crown ether. Not surprisingly, Ba−C(π) interactions from each barium center were observed with only one of the enolate systems, with values ranging from 3.166(5) to 3.426(5) Å (Table 7). The exposed face of each barium is capped by a THF molecule. Also, a product of the desilylation pathway, the strontium enolate $[\{Sr(18\text{-crown-}6)(OC_2H_3)\}_2][CHPh_2]_2$,[61] is a doubly enolate-bridged diphenylmethanide dimer, with the metal ions lying above the plane of the crown ether and tipped toward each other on one face. Reflecting the smaller ionic radii of the metal (Table 1), no Sr−C(π) interactions were observed with the enolate moieties. The diphenylmethanide anion displays a "50/50 flip" disorder.[61,64,103]

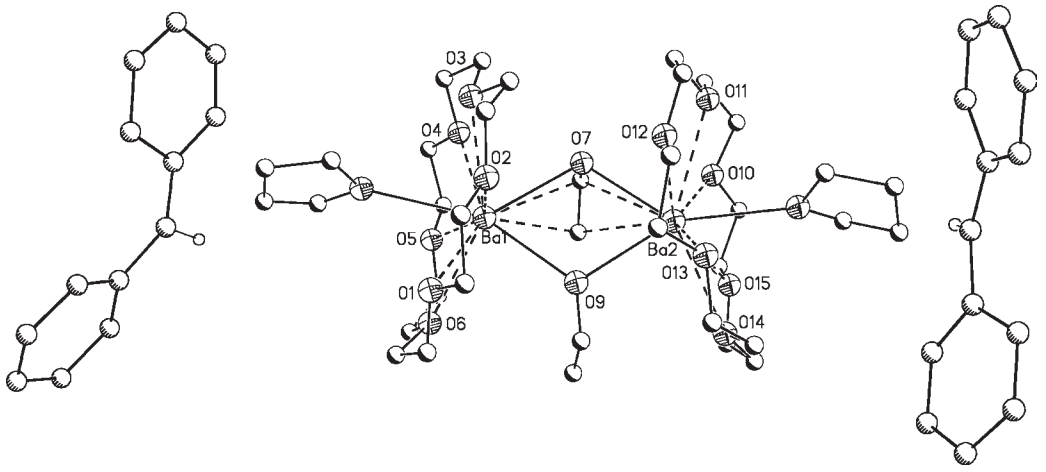

Figure 15. Crystal structure of $[\{Ba(18\text{-crown-6})(OC_2H_3)(thf)\}_2][CHPh_2]_2$.[61] Nonbenzylic hydrogen atoms are omitted for clarity.

Table 7. Selected Bond Lengths for Alkaline-Earth-Metal Diphenylmethanides

	CN	hapticity of the ligand	M−C_α (Å)	M−donor (Å)[a]	M−C(π) (Å)	ref
$[\{Sr(18\text{-crown-6})(OC_2H_3)\}_2][CHPh_2]_2$	8			2.674(3)[a]		61
				2.397(3)[b]		
$Ba(CHPh_2)_2(dme)_2$	10	η^2, η^4	2.902(4)	2.755(2)	3.021(1)−3.437(1)	64
$Ba(CHPh_2)_2(18\text{-crown-6})$	9	η^1, η^2	3.081(3)	2.778(3)	3.389(3)	61
$[Ba(hmpa)_6][CHPh_2]_2$	6			2.633(3)		64
$[\{Ba(18\text{-crown-6})(OC_2H_3)(thf)\}_2][CHPh_2]_2$	11			2.869(3)[a]	3.166(5)−3.426(5)	61
				2.685(3)[b]		
				2.868(3)[c]		

[a] a = crown; b = enolate; c = thf; d = diglyme.

Toluene elimination also afforded the two barium coligand adducts $Ba(CHPh_2)_2(dme)_2$[64] and $[Ba(hmpa)_6][CHPh_2]_2$,[61] where the impact of the coligand on the structural features was demonstrated. The addition of the strong donor HMPA results in complete ion separation, whereas the use of DME results in the σ-bonded contact molecule. The $[Ba(hmpa)_6]^+$ cation along with $[M(18\text{-crown-6})(hmpa)_2]^+$ (M = Sr, Ba) demonstrates the ability of crown and HMPA to reliably promote ion separation of the heavy alkaline-earth metals.[27,62,107,113]

$Ba(CHPh_2)_2(dme)_2$ (Figure 16) nicely showcases the difficulties in predicting metal−ligand bonding because two different metal−ligand bonding modes are observed within the same molecule.[64] Each ligand coordinates to the metal center through Ba−C_α σ bonds [2.89(4)−3.04(2) Å], which are slightly shorter than those found in $Ba(CHPh_2)_2(18\text{-crown-6})$ [3.065(3)−3.096(3) Å].[64] Metal coordinative saturation was achieved by a range of Ba−C(π) interactions, as shown in Figure 16, ranging from 3.021(1) to 3.437(1) Å.

Addressing the solubility limitation of benzyl-based compounds, substitution at C_α generally improves the solubility while affording compounds capable of increased coordinative saturation. In the interest of space, only selective examples will be discussed, but many phosphorus-substituted[114−117] and silicon[97−101,118−130] benzyl-based compounds have been reported.

Despite the availability of a viable synthetic route in alkane elimination with the widely available $^n Bu_2Mg$ (Scheme 2b, route i), no magnesium diphenylmethanides have been disseminated. However, an example based on variation of the diphenylmethanide ligand, α-$MeCH_2Ph$, where one of the phenyl groups has been replaced by a methyl, has been reported, $Mg(MeCHPh)_2(Et_2O)_2$ (Table 8).[131] Substitution at C_α with a pyridyl group

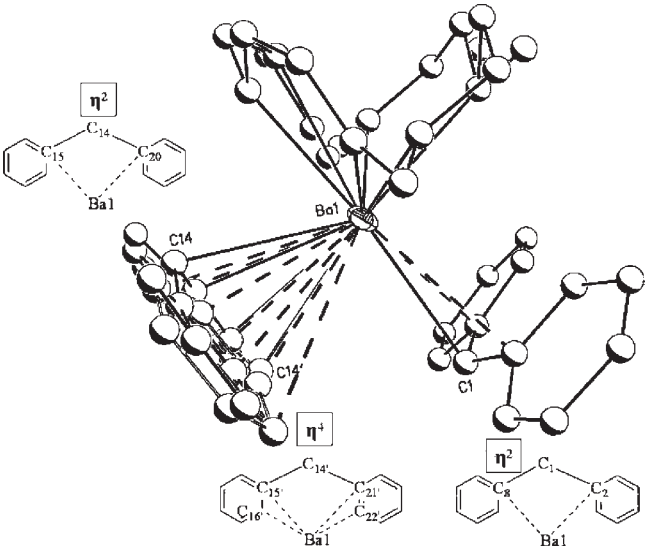

Figure 16. Illustration of $Ba(CHPh_2)_2(dme)_2$ showing all disorder positions in DME and diphenylmethanide "flip" positions (C_α carbons are C14 and C14′).[64] Ba−C(π) interactions are shown as dotted lines. Hydrogen atoms are omitted for clarity.

Table 8. Selected Bond Lengths for s-Block α-Substituted Benzyl-Based Alkali- and Alkaline-Earth-Metal Compounds

	CN	hapticity of the ligand	M−C_α (Å)	M−donor (Å)[a]	M−C(π) (Å)	ref
$Mg(MeCHPh)_2(Et_2O)_2$	4	η^1	2.057(10)	2.195(11)		131
Li(DMAT)(tmeda)	6	η^4	2.219(6)	2.143(7)[a]	2.421(6)−2.449(7)	97
				2.052(2)		
$Ca(DMAT)_2(thf)_2$	10	η^4	2.628(3)	2.599(3)[a]	3.078(2)−3.140(3)	99
				2.407(2)		
$Sr(DMAT)_2(thf)_2$	10	η^4	2.782(2)	2.771(2)[a]	2.862(2)−3.019(2)	97
				2.546(2)		
$[K(DMAT)(thf)]_\infty$	11	$\mu-\eta^6:\eta^3$	2.966(4)	2.906(4)[a]	3.027(3)−3.532 (3)	97
				2.633(4)		
$Ba[CHPh(C_5H_3N\text{-}2)]_2(diglyme)(thf)$	14	η^5	3.142(4)	2.807(5)[b]	2.982(5)−3.303(5)	132
				2.819(4)[c]		

[a] a = $-NMe_2$; b = THF; c = diglyme.

allowed isolation of the η^5-coordinate contact molecule $Ba[CHPh(C_5H_3N\text{-}2)]_2(diglyme)(thf)$ through the reaction of barium metal in liquid ammonia in the presence of 2-pyridylphenylmethane and diglyme (Scheme 2b, route vi).[132] For this compound, the pyridyl group acts as an intramolecular Lewis base, further stabilizing the metal center. Similar to previous diphenylmethanide anions, the 2-pyridylphenylmethane anions display a "flip" disorder, with Ba−C(π) interactions ranging from 2.982(5) to 3.303(5) Å (Table 8). Intramolecular metal stabilization was also achieved through the introduction of methylamino groups into the benzyl ring in the ligands 2-NMe_2-α-$Me(CH_2Ph)$ and 2-NMe_2-α-$SiMe_3(CH_2Ph)$. The addition of the methylamino group into the benzyl ring allowed for isolation of $Ca[2\text{-}NMe_2\text{-}\alpha\text{-}MeCHPh]_2(thf)_2$, where each ligand is η^2-coordinate, binding through C_α and the neutral methylamino group.[130] However, the compound was found to display poor solubility, and reliable structural data were unavailable.

Substitution of C_α with a $-SiMe_3$ group in the ligand 2-NMe_2-α-$SiMe_3(CH_2Ph)$, referred to as DMAT, afforded a series of both alkali- and alkaline-earth-metal species that displayed increased solubility and proved good utility as polymerization initiators.[97−101] The TMEDA-solvated lithium compound, Li(DMAT)(tmeda), shows a monomeric four-coordinate metal center with an η^4-coordinate ligand (Scheme 2a, route i).[97] In addition to binding to C_α and the methylamino group, two additional Li−C(π) interactions arise to stabilize the metal center (Table 8). Consistent with the larger metal radius, the potassium species, $[K(DMAT)(thf)]_\infty$, displays a polymeric structure, despite THF coordination.[97] The linear coordination polymer is propagated through intermolecular K−η^6-C(π) interactions between the phenyl group and the adjacent metal unit. Similar to the lithium species, the ligand is η^4-coordinate; however, additional metal saturation is achieved through K···H−C interaction (3.24 Å) from one of the $-SiMe_3$ groups.

Salt metathesis (Scheme 2b, route ii) allowed the preparation of $Ca(DMAT)_2(thf)_2$[88] and $Sr(DMAT)_2(thf)_2$.[97,99] Both species display η^4 metal coordination to the ligand and, similar to the lithium and potassium species, are comprised of metal−ligand contacts with C_α on the methylamino group and two additional M−C(π) interactions, as summarized in Table 8. Consistent with the smaller ionic radius, Ca−C_α [2.628(3) Å] is shorter than Sr−C_α [2.782(2) Å]; however, the M−C(π) interactions for the strontium species were relatively shorter compared to those of the calcium compound (Table 8).

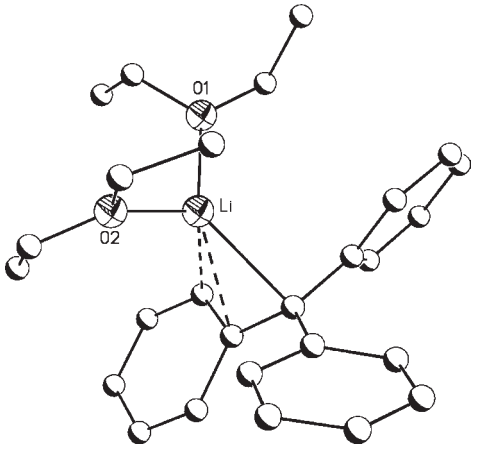

Figure 17. Crystal structure of $Li(CPh_3)(Et_2O)_2$.[133] All hydrogen atoms are omitted for clarity.

6. TRIPHENYLMETHANE LIGAND

While slightly bulkier than the diphenylmethanides, because of the presence of an additional phenyl group, triphenylmethanide species can be obtained using reaction conditions similar to those applied toward the diphenylmethanides. Nonetheless, the ligand's capacity for metal−σ bonds might decrease because of steric hindrance from the phenyl groups. In this respect, donor studies revealed preferred geometries and coordination motifs of the ligand and its effect on how metal stabilization is achieved. While the diphenylmethanide anion $[CHPh_2]^-$ typically displays planarity once deprotonated, the triphenylmethanide anion $[CPh_3]^-$ adopts a propeller-like geometry. Because the trigonal-planar geometry does not provide sufficient space for three planar phenyl groups, the rings are canted toward each other by an average of 25°.[104]

Metalation of triphenylmethanide can be achieved through the use of either alkyllithium or alkylsodium, as described above for diphenylmethanides (Scheme 2a, route i). In the presence of Et_2O and TMEDA, η^3 coordination is observed for $Li(CPh_3)(Et_2O)_2$[133] (Figure 17), while η^4 coordination is found in $Li(CPh_3)(tmeda)$,[134] with Li−C_α distances of 2.306(14) and 2.227(8) Å, respectively. Additional Li−C(π) interactions are observed for both complexes and summarized in Table 9. Both anions adopt a propeller-like geometry. A similar

Table 9. Selected Bond Lengths for Alkali-Metal Triphenylmethanides

	CN	hapticity of the ligand	M−C_α (Å)	M−donor (Å)[a]	M−C(π) (Å)	ref
$Li(CPh_3)(Et_2O)_2$	5	η^3		1.933(13)	2.306(14)−2.868(14)	133
$[Li(thf)_4][CPh_3]$	4			1.901(3)		136
$Li(CPh_3)(tmeda)$	6	η^4		2.075(9)	2.227(8)−2.541(9)	134
$[Li(12\text{-crown-}4)_2][CPh_3]$	8		2.365(2)			104
$[Na(CPh_3)(tmeda)]_\infty$	8	$\mu-\eta^5:\eta^1$	2.643(3)	2.451(3)	2.886(1)−3.088(1)	135
$[K(CPh_3)(thf)]_\infty$	11	$\mu^3-\eta^6:\eta^3:\eta^1$	3.003(9)	2.624(8)	3.105(3)−3.292(3)	137
$[K(CPh_3)(diglyme)]_\infty$	13	$\mu-\eta^5:\eta^5$	3.016(2)	2.717(2)	3.153(3)−3.547(2)	137
$K(CPh_3)(pmdta)$	10	η^7	2.931(3)	2.869(3)	3.048(3)−3.507(3)	137
$K(CPh_3)(pmdta)(thf)$	10	η^6		2.836(4)[a]	3.142(4)−3.253(4)	138
				2.721(4)[b]		
$[Rb(CPh_3)(pmdta)]_\infty$	15	$\mu-\eta^6:\eta^6$		3.090(7)	3.351(4)−3.643(3)	138
$[Cs(CPh_3)(dme)_2]_\infty$	16	$\mu-\eta^7:\eta^6$	3.272(2)	3.103(2)	3.479(2)−3.696(2)	145
$[Cs(CPh_3)(pmdta)]_\infty$	16	$\mu-\eta^7:\eta^6$	3.334(8)	3.262(4)	3.434(4)−3.820(4)	138

[a] a = nitrogen-based donor; b = oxygen-based donor.

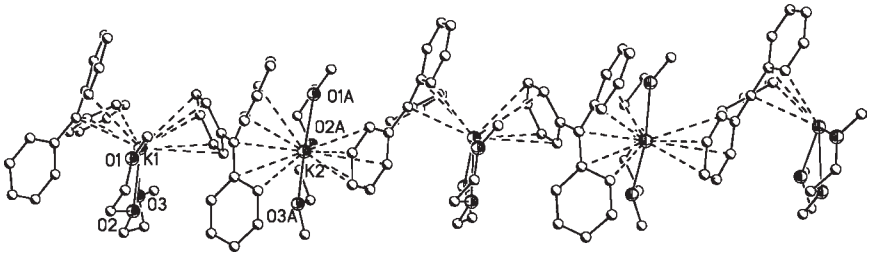

Figure 18. Crystal structure of $[K(CPh_3)(diglyme)]_\infty$.[137] All hydrogen atoms are omitted for clarity.

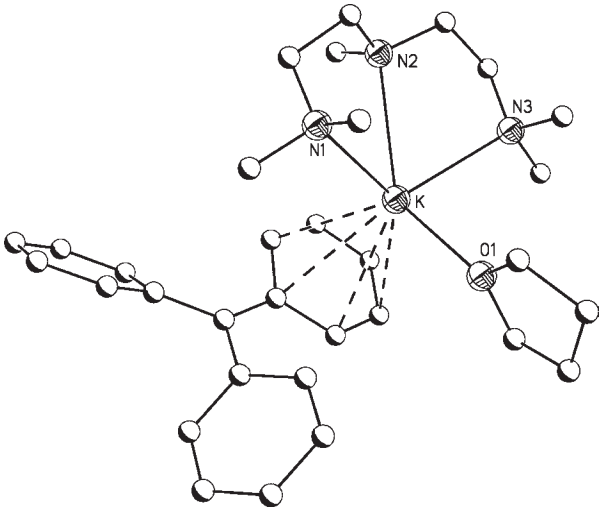

Figure 19. Crystal structure of $K(CPh_3)(pmdta)(thf)$.[138] K−C(π) interactions are shown as dotted lines. Hydrogen atoms are omitted for clarity.

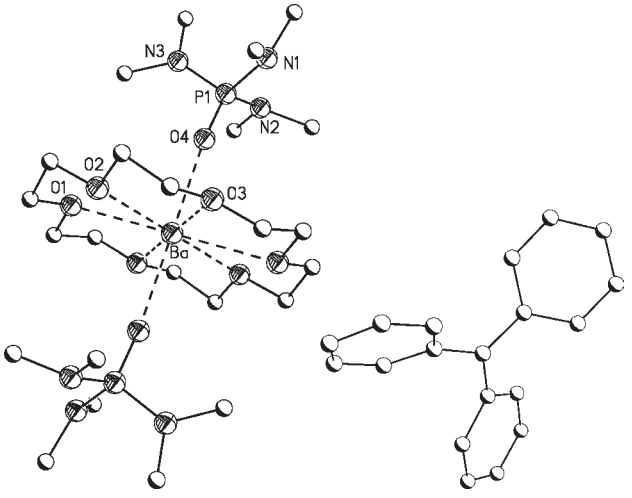

Figure 20. Crystal structure of $[Ba(18\text{-crown-}6)(hmpa)_2][CPh_3]_2$.[64] Only one triphenylmethanide anion is shown. Hydrogen atoms are omitted for clarity.

structural motif is observed for $[Na(CPh_3)(tmeda)]_\infty$[135] with an η^5 ligand coordination mode with a Na−C_α distance of 2.643(3) Å. In addition to the intramolecular interactions from the coordinated ligand, an additional intermolecular Na−C(π) interaction arises from a phenyl group from a neighboring unit, resulting in a coordination polymer (Table 9).

Similar to the ion-separated diphenylmethanide, $[Li(12\text{-crown-}4)_2][CHPh_2]$,[104] ion separation is also observed for the triphenylmethanide derivative, $[Li(12\text{-crown-}4)_2][CPh_3]$.[104] In both cases, complete encapsulation of the metal cation is achieved by two 12-crown-4 macrocycles, resulting in a sandwiched lithium metal center. This coordination provides effective steric saturation, and no Li−C(π) interactions are observed.

dx.doi.org/10.1021/ic201148d |*Inorg. Chem.* 2011, 50, 12223–12240

Table 10. Selected Bond Lengths for Alkaline-Earth-Metal Triphenylmethanides

	CN	hapticity of the ligand	M−C_α (Å)	M−donor (Å)[a]	ref
$Mg(CPh_3)(Br)(Et_2O)_2$	4	η^1	2.250(1)	2.031(1)	148
$[Ca(thf)_6][CPh_3]_2$	6			2.336(3)	57
$[Sr(18\text{-crown-6})(hmpa)_2][CPh_3]_2$	8			2.409(2)[a]	65
				2.707(2)[b]	
$[Ba(hmpa)_6][CPh_3]_2$	6			2.642(4)	64
$[Ba(18\text{-crown-6})(hmpa)_2][CPh_3]_2$	8			2.587(2)[a]	62
				2.785(2)[b]	

[a] a = hmpa; b = crown.

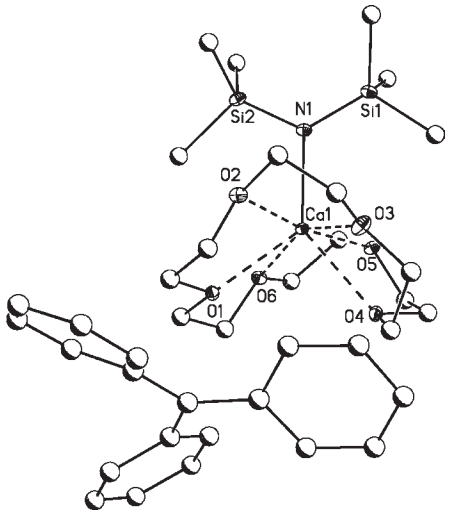

Figure 21. Crystal structure of $[Ca(N(SiMe_3)_2)(18\text{-crown-6})][CPh_3]$.[64] Hydrogen atoms are omitted for clarity.

THF coordination has also shown to be effective to coordinatively stabilize the metal center and induce ion dissociation, as seen in $[Li(thf)_4][CPh_3]$.[136]

As discussed previously, the synthesis of the heavier metal congeners is hampered by the limited availability of easily synthesized and soluble starting materials. However, the reaction of ^{n}BuLi and MO^{t}Bu (M = K−Cs; Scheme 2a, route iv), shown to be successful toward benzylate derivatives,[57,58] allowed for the preparation of $[CPh_3]^-$ complexes. In addition to this "superbase" reaction route, potassium metal is a viable starting material (Scheme 2a, route ii), as shown by the isolation of three contact species, $[K(CPh_3)(thf)]_\infty$, $[K(CPh_3)(diglyme)]_\infty$, and $K(CPh_3)(pmdta)$.[137] $[K(CPh_3)(thf)]_\infty$ with $[K(CPh_3)(diglyme)]_\infty$ both crystallize as coordination polymers propagated by inter- and intramolecular K−C(π) interactions. In $[K(CPh_3)(diglyme)]_\infty$, the ligand is η^5-coordinate with a K−C_α distance of 3.016(2) Å, while five additional K−C(π) interactions arise from the phenyl group of a neighboring unit, propagating the coordination polymer (Figure 18). In $[K(CPh_3)(thf)]_\infty$, coordination of the smaller THF donor results in an overall higher coordination number for the metal center and aggregation into a two-dimensional coordination polymer. In this case, a K−C_α distance of 3.004(3) Å is observed for the ligand bound in an η^3 motif with two additional intramolecular interactions [3.105(3) and 3.168(3) Å]. A neighboring anion saturates the metal center with further η^6 coordination from one of its phenyl groups [3.164(3)−3.292(3) Å]. Finally, the same anion bridges a metal center through an additional K−C(π) interaction [3.172(3) Å; Table 9]. Demonstrating the role of the coligand, the tridentate PMDTA affords the monomeric contact species $K(CPh_3)(pmdta)$.[137] In this case, the metal center is saturated by K−C(π) interactions from the η^7-coordinate ligand with a K−C_α distance of 2.931(3) Å and additional intramolecular interactions ranging from 3.048(3) to 3.507(3) Å (Table 9). In addition, three agostic interactions stemming from the PMDTA molecule arise to coordinatively saturate the metal center, with values ranging from 3.128(3) to 3.276(3) Å.

Table 11. Selected Bond Lengths for Benzyl-Based Monocationic Calcium Species

	CN	M−N (Å)	M−O (Å)	ref
$[Ca(N(SiMe_3)_2)(18\text{-crown-6})][CHPh_2]$	7	2.311(3)	2.530(3)	64
$[Ca(N(SiMe_3)_2)(18\text{-crown-6})][CPh_3]$	7	2.317(3)	2.512(2)	64

Interestingly, reactions of KO^{t}Bu and $CHPh_3$ with PMDTA under "super-base" conditions in THF (Scheme 2a, route iv) result in the monomeric species $K(CPh_3)(pmdta)(thf)$ (Figure 19), where the coordination of THF dramatically effects the coordination motif of the ligand.[138] Despite having the same overall coordination number of 10, a direct K−C_α bond is not observed, but rather η^6 coordination to one of the phenyl groups aids in stabilizing the metal center (Table 9).[138] As the metal size increases to rubidium and cesium, the preference for M−C(π) interactions increases even in the presence of donor molecules such as THF,[139−144] and the metal coordination sites are occupied almost entirely by these interactions. In $[M(CPh_3)(pmdta)]_\infty$ (M = Rb, Cs),[138] coordination of the multidentate PMDTA donor does not circumvent aggregation. The rubidium species has an overall metal coordination number of 15, flanked on either side by η^6-coordinated phenyl groups from the anion, which also coordinate to neighboring metal centers, propagating a coordination polymer through Rb−C(π) interactions (Table 9). The larger cesium metal center has an overall coordination number of 16. Despite η^7 coordination to one ligand with a Cs−C_α distance of 3.334(8) Å, a neighboring phenyl group η^6-coordinates to the metal center, propagating the coordination polymer (Table 9).

Finally, the reaction of cesium metal in DME afforded the 16-coordinate polymeric species $[Cs(CPh_3)(dme)_2]_\infty$ (Scheme 2a, route ii).[145] Similar to $[Cs(CPh_3)(pmdta)]_\infty$,[138] the coordination polymer is propagated by two distinct ligand coordination motifs, η^6-coordinate through a phenyl group, and an η^7-coordinated ligand with a Cs−C_α distance of 3.272(2) Å. Cs−C(π) interactions are summarized in Table 9. Curiously, one DME molecule is coordinated to one metal center, while the second DME molecule is bridging two neighboring cesium

Table 12. Selected Bond Lengths for s-Block α-Substituted Triphenylmethanides

	CN[a]	hapticity of the ligand[a]	M−C$_\alpha$ (Å)	M−donor (Å)[a]	M−C(π) (Å)	ref
$[Li(thf)_4][Li(SiMe_2PhCPh_2)_2]$	8	η^4	2.125(2)	1.912(2)	2.356(2)−2.658(2)	111
	4					
$[Li(thf)_4][Li(SiMe_3CPh_2)_2]$	10[x]	η^{5y}	2.141(2)	1.925(2)	2.414(2)−2.802(2)	111
	4[y]					
$[Li(tmeda)_2][SiMe_3CPh_2]$	4			2.143(7)		111
$Li(PyrCPh_2)(Et_2O)_2$	5	η^3		1.932(3)[a]	2.444(2)−2.833(3)	157
				1.972(3)[b]		
$Na(SiMe_3CPh_2)(pmdta)$	6	η^3	2.690(5)	2.474(4)	2.631(5)−2.784(5)	129
$Na(PyrCPh_2)(thf)_3$	6	η^3		2.335(2)[a]	2.859(2)−3.067(2)	157
				2.413(2)[b]		
$Ca[(SiMe_3)_2CPh]_2(thf)_2$	8	η^3	2.649(2)	2.381(2)	2.893(2)−2.960(2)	158
$K(PyrCPh_2)(pmdta)(thf)$	8	η^4		2.906(4)[a]	3.140(2)−3.454(2)	157
				2.809(3)[b]		
				2.746(3)[c]		
$[K[(SiMe_3)_2CPh]]_\infty$	9	$\mu-\eta^6:\eta^3$	3.007(3)		3.092(2)−3.522(2)	158
$[K(18\text{-crown-}6)][C(C_6Cl_5)_3]$	6			2.771(1)		159

[a] x = cation; y = anion; a = oxygen-based donor; b = pyridyl; c = nitrogen-based donor.

centers located on adjacent polymeric chains, creating a two-dimensional structure.

As discussed previously for diphenylmethanide species, $[M(hmpa)_6]^+$ and $[M(18\text{-crown-}6)(hmpa)_2]^+$ (M = Sr, Ba) are well-reported cations supporting ion separation,[23,26,27,29,62,65,107,113,146] a motif also observed for the triphenylmethanide derivatives $[M(18\text{-crown-}6)(hmpa)_2][CPh_3]_2$ (M = Sr, Ba)[62,65] (Figure 20) and $[Ba(hmpa)_6][CPh_3]_2$ (Table 10).[64] All were prepared using the toluene elimination route (Scheme 2b, route v). The $[CPh_3]^-$ anions display a propeller-like geometry without additional M−C(π) interactions. For the smaller metal calcium, THF coordination alone is sufficient to induce ion separation as observed in $[Ca(thf)_6][CPh_3]_2$, afforded through salt metathesis (Scheme 2, route i).[57] The crystal packing for this species has been described as a "metal-in-a-box" model, previously reported for other solvent-separated ion pairs of the alkaline-earth metals.[147]

For magnesium, reactions of triphenylmethyl bromide with activated magnesium in a diethyl ether/benzene mixture afforded heteroleptic contact molecule $Mg(CPh_3)(Br)(Et_2O)_2$.[148] The η^1-coordinated ligand displays a Mg−C$_\alpha$ distance of 2.250(1) Å (Table 10). The ligand is arranged in a propeller-like geometry without additional Mg−C(π) interactions.

Transmetalation (Scheme 2, route iv) allowed the preparation of two monocationic species, $[Ca(N(SiMe_3)_2)(18\text{-crown-}6)][CHPh_2]$ and $[Ca(N(SiMe_3)_2)(18\text{-crown-}6)][CPh_3]$ (Figure 21), in THF or DME at −78 °C.[64] Remarkably, these were obtained by treating $Ca[N(SiMe_3)_2]_2(thf)_2$ with the lithium organometallics in either 1:1, 1:2, 1:3, or 1:4 ratios (Scheme 2b, route iii), none of which led to the anticipated dication $[Ca(18\text{-crown-}6)(thf)_2]^{2+}$, despite previous reports of a $[Ca(thf)_6]^{2+}$ or a $[Ca(18\text{-crown-}6)(hmpa)_2]^{2+}$ cation formulation in other separated complexes.[27,29,57,147,149−151] In all instances where excess lithium reagent was utilized, a mixture with unreacted organolithium reagent was identified. With the driving force for transmetalation reactions being the precipitation of one of the two solid products, the reproducible precipitation of these monocations provides a rationale for this observation. Furthermore, the significant polar bond character of the target compounds renders coordinative saturation a major structure deciding factor, suggesting a favorable calcium environment based on amide and crown ether coordination. This assumption is further supported by the contact molecule $Ba(CHPh_2)_2(18\text{-crown-}6)$, where the larger barium center supports the coordination of crown ether in addition to two diphenylmethanides (Figure 14).[61]

The monocationic species display identical cation structures, with $[N(SiMe_3)_2]^-$ and crown ether coordinating to the metal center, resulting in a coordination number of 7. The crown is severely puckered. Interestingly, the Ca−O crown distances in the $[CPh_3]^-$ derivative fall in a narrow range [2.472(2)−2.512(2) Å], whereas those for the $[CHPh_2]^-$ species vary more [2.370(8)−2.691(3) Å; Table 11]. Previous examples of $[Ca(18\text{-crown-}6)]^{2+}$ have clearly shown calcium to be too small for the crown cavity, with the metal center typically not located in the center of the crown, as seen in $[Ca(NH_3)_3(18\text{-crown-}6)][S\text{-}2,4,6\text{-}{}^tBu_3C_6H_2]_2$, with Ca−O(crown) distances ranging from 2.421(3) to 2.964(4) Å).[146] The puckered arrangement alleviates this problem, as seen by the narrow range of Ca−O distances in $[CPh_3]^-$, but also allows for a rather flexible crown geometry, as demonstrated by the $[CHPh_2]^-$ derivative. Showing the flexibility of the coordination environment, the $[CPh_3]^-$ derivative is highly disordered, involving amide and crown ether along with the separated anion.

The Ca−N bond lengths for the seven-coordinate monocationic $[Ca(N(SiMe_3)_2)(18\text{-crown-}6)][CHPh_2]$ [2.311(3) Å] and $[Ca(N(SiMe_3)_2)(18\text{-crown-}6)][CPh_3]$ [2.317(3) Å] are short and are in close agreement with the four-coordinate $Ca[N(SiMe_3)_2]_2(donor)_n$ {where donor = THF, n = 2 [Ca−N 2.301(6) Å];[152] pyr, n = 2 [Ca−N 2.321(1) Å];[153] TMEDA, n = 1 [Ca−N 2.328(1) Å]}[153] or the three-coordinate dimer $[Ca\{N(SiMe_3)_2\}_2]_2$ [Ca−N$_{terminal}$ 2.28(1) Å; Ca−N$_{bridging}$ 2.48(2) Å].[154] The similar values of the Ca−N distances are likely a consequence of the cationic nature of the fragment.

In analogy to the separated $[CHPh_2]^-$ and $[CPh_3]^-$ complexes described above, the anions for both monocationic species are resonance-stabilized, as represented by the planar geometry of the central carbon atoms. The $[CPh_3]^-$ anion represents C$_i$−C$_\alpha$−C$_i$ angles close to the ideal trigonal-planar geometry

[119.5(3), 119.7(3), and 120.9(3)°]. For the $[CHPh_2]^-$ anion, the presence of a hydrogen atom instead of a phenyl group results in significant widening of the $C_i-C_\alpha-C_i$ angle to 134.7(13) and 148.0(13)°. Canting angles in the more congested $[CPh_3]^-$ anion range from 24.4 to 34.0°; again, they are smaller (between 0.4 and 6.5°) for the less constrained $[CHPh_2]^-$.

While all di- and triphenylmethanides are highly reactive, comparative observation of the reactivity of the monocationic calcium species $[Ca(N(SiMe_3)_2)(18\text{-crown-}6][CHPh_2]$ and $[Ca(N(SiMe_3)_2)(18\text{-crown-}6][CPh_3]$ shows them to be significantly more reactive, clearly a consequence of the flexible metal coordination, because previous examples of monocationic calcium-based complexes, $[(C_5Me_5)Ca(OPPh_3)_3][I]$[155] and $[Me_2P(2\text{-Me-}4\text{-}^tBu\text{-}C_5H_2)_2Ba(thf)_3][BPh_4]$,[156] did not report increased reactivity.

While many substituted triphenylmethane s-block species have been reported,[111,129,157−160] only selected examples will be discussed in the interest of space. Substitution of triphenylmethane at C_α with a pyridyl group allowed isolation of a family of alkali-metal compounds, $Li(PyrCPh_2)(Et_2O)_2$ (Scheme 2a, route i), $Na(PyrCPh_2)thf)_3$, and $K(PyrCPh_2)(pmdta)(thf)$ (Scheme 2a, route iv).[157] With an increase in the metal size, both the hapticity of the ligand and the overall coordination numbers increase (Table 12). The addition of the pyridyl group afforded additional intramolecular stabilization and effectively reduced aggregation compared to previously discussed polymeric species $[M(CPh_3)(donor)]_\infty$ (M = Na−Cs).[135,137,138,145]

Ion-separated lithium triphenylmethanide species were obtained by replacing one of the phenyl groups by silyl substituents at C_α. The $-SiMe_3$-substituted ligand α-$SiMe_3CHPh_2$ afforded the separated species $[Li(tmeda)_2][SiMe_3CPh_2]$ and $[Li(thf)_4][Li(SiMe_3CPh_2)_2]$ (Scheme 2a, route i)[111] and the contact species $Na(SiMe_3CPh_2)(pmdta)$ (Scheme 2a, route iv).[129] In the $[Li(thf)_4][Li(SiMe_3CPh_2)_2]$ lithiate species, two $[SiMe_3CPh_2]^-$ anions are σ-bonded to the lithium metal center [2.141(2) Å] and stabilize the metal center through four additional $Li-C(\pi)$ interactions from the phenyl groups ranging from 2.414(2) to 2.802(2) Å (Table 12). A similar lithiate $[Li(thf)_4][Li(SiMe_2PhCPh_2)_2]$ (Scheme 2a, route i) was obtained with the use of α-$SiMe_2PhCHPh_2$,[111] where two anions are σ-bonded to the lithium metal center [2.125(2) Å] and stabilize the metal center through three additional $Li-C(\pi)$ interactions from the phenyl groups ranging from 2.356 to 2.658(2) Å (Table 12). $Na(SiMe_3CPh_2)(pmdta)$ displays a $Na-C_\alpha$ of 2.690(5) Å and three additional $Na-C(\pi)$ interactions ranging from 2.631(5) to 2.784(5) Å (Table 12) resulting in η^3 coordination.[129]

Substitution of triphenylmethane at C_α with two $-SiMe_3$ groups results in the ligand α,α-$(SiMe_3)_2CHPh$, which has been used to afford the polymeric $[K[(SiMe_3)_2CPh]]_\infty$ (Scheme 2a, route iv) and the contact species $Ca[(SiMe_3)_2CPh]_2(thf)_2$ (Scheme 2b, route ii).[158] $[K[(SiMe_3)_2CPh]]_\infty$ is propagated through intermolecular $K-\eta^6$-$C(\pi)$ interactions between the phenyl group and the adjacent metal unit similar to the above-mentioned $[K(DMAT)(thf)]_\infty$.[97] The ligand coordinates in an η^3 fashion, with additional metal saturation achieved via neighboring units through K···H−C interactions from the $-SiMe_3$ groups [3.001(3) Å]. $Ca[(SiMe_3)_2CPh]_2(thf)_2$ displays η^3 coordination to each ligand with a $Ca-C_\alpha$ distance of 2.649(2) Å. Two additional $Ca-C(\pi)$ interactions arise in order to fully saturate the metal center (Table 12). Finally, complete ion separation for potassium was achieved by introducing perchlorotriphenylmethane in the presence of 18-crown-6 in $[K(18\text{-crown-}6)][C(C_6Cl_5)_3]$.[159] No $K-C(\pi)$ interactions were reported.

7. CONCLUSIONS

The chemistry of benzyl-based s-block organometallics has seen significant progress because of advances in synthetic protocols providing many insights for the further development of s-block organometallic chemistry. Despite the progress, the prediction of the molecular geometry remains challenging because a range of metal−ligand binding modes, along with a propensity of noncovalent interactions, provide a variety of structural possibilities all within a narrow energetic range.

AUTHOR INFORMATION

Corresponding Author

*E-mail: kruhland@syr.edu. Telephone: 1-315-443-1306. Fax: 1-315-443-4070.

ACKNOWLEDGMENT

The authors gratefully acknowledge support from the National Science Foundation (Grant CHE 0753807) and Syracuse University.

REFERENCES

(1) Elschenbroich, C. *Organometallics*; Wiley-VCH Verlag GmnH & Co., KGaA: Weinheim, Germany, 2006.
(2) Smith, J. D. *Adv. Organomet. Chem.* **1999**, *43*, 267.
(3) Alexander, J. S.; Zuniga, M. F.; Guino-o, M. A.; Hahn, R. C.; Ruhlandt-Senge, K. The Organometallic Chemistry of the Alkaline Earth Metals. *The Encyclopedia of Inorganic Chemistry*; Wiley: New York, 2006; Vol. 1, p 116.
(4) Schlenk, W.; Marcus, E. *Ber. Dtsch. Chem. Ges.* **1914**, *47*, 1664.
(5) Schlenk, W.; Bergmann, E.; Benedikt, B.; Blum, O.; Bresiewicz, C.; Rodloff, I.; Appenrodt, J.; Ehninger, K.; Ender, H.; Israel, R.; Knorr, A.; Kohler, T.; Michael, A.; Muller, E.; Rubens, E.; Schmidt-Nickels, W.; Stoffers, W.; Wiegandt, A.; Willstadt, H. *Ann.* **1928**, *464*, 1.
(6) Reich, H. J. http://www.chem.wisc.edu/areas/reich/pkatable/index.htm.
(7) Ripin, D.; Evans, D. http://daecr1.harvard.edu/pKa/pKa.html.
(8) Buncel, E.; Menon, B. *J. Chem. Soc., Chem. Commun.* **1978**, *17*, 758.
(9) Buncel, E.; Menon, B. *J. Org. Chem.* **1979**, *44* (3), 317.
(10) Buncel, E.; Menon, B. C.; Colpa, J. P. *Can. J. Chem.* **1979**, *57* (9), 999.
(11) Menon, B.; Buncel, E. *J. Organomet. Chem.* **1978**, *159* (4), 357.
(12) Menon, B. C.; Shurvell, H. F.; Colpa, J. P.; Buncel, E. *J. Mol. Struct.* **1982**, *78* (1−2), 29.
(13) Lambert, C.; Schleyer, P. v. R. *Angew. Chem.* **1994**, *106*, 1187.
(14) Shannon, R. D. *Acta Crystallogr., Sect. A* **1976**, *A32*, 751.
(15) Westerhausen, M. *Coord. Chem. Rev.* **1998**, *176*, 157.
(16) Harder, S. *Organometallics* **2002**, *21*, 3782.
(17) Torvisco, A.; Decker, K.; Uhlig, F.; Ruhlandt-Senge, K. *Inorg. Chem.* **2009**, *48*, 11459.
(18) Chen, H.; Bartlett, R. A.; Rasika Dias, H. V.; Olmstead, M. M.; Power, P. P. *J. Am. Chem. Soc.* **1989**, *111*, 4338.
(19) Bartlett, R. A.; Olmstead, M. M.; Power, P. P. *Inorg. Chem.* **1994**, *33*, 4800.
(20) Westerhausen, M.; Gärtner, M.; Fischer, R.; Langer, J. *Angew. Chem., Int. Ed.* **2007**, *46* (12), 1950.
(21) Bartlett, R. A.; Power, P. P. *J. Am. Chem. Soc.* **1987**, *109* (12), 6509.

(22) Hitchcock, P. B.; Khvostov, A. V.; Lappert, M. F.; Protchenko, A. V. *J. Organomet. Chem.* **2002**, *647*, 198.
(23) Teng, W.; Englich, U.; Ruhlandt-Senge, K. *Angew. Chem., Int. Ed.* **2003**, *42* (31), 3661.
(24) Alexander, J. S.; Ruhlandt-Senge, K. *Angew. Chem., Int. Ed.* **2001**, *40*, 2658.
(25) Alexander, J. S.; Ruhlandt-Senge, K.; Hope, H. *Organometallics* **2003**, *22*, 4933.
(26) Ruhlandt-Senge, K.; Englich, U. *Chem.—Eur. J.* **2000**, *6*, 4063.
(27) Englich, U.; Ruhlandt-Senge, K. *Z. Anorg. Allg. Chem.* **2001**, *627*, 851.
(28) Chadwick, S.; Englich, U.; Ruhlandt-Senge, K. *Chem. Commun.* **1998**, 2149.
(29) Englich, U.; Ruhlandt-Senge, K.; Uhlig, F. *J. Organomet. Chem.* **2000**, *613*, 139.
(30) Chadwick, S.; Englich, U.; Ruhlandt-Senge, K. *Inorg. Chem.* **1999**, *38*, 6289.
(31) Jaenschke, A.; Paap, J.; Behrens, U. *Z. Anorg. Allg. Chem.* **2008**, *634*, 461.
(32) Torvisco, A.; Ruhlandt-Senge, K. *Organometallics* **2011**, *30*, 986.
(33) Allred, A. L.; Rochow, E. G. *J. Inorg. Nucl. Chem.* **1958**, *5*, 264.
(34) Pedersen, C. J. *J. Am. Chem. Soc.* **1967**, *89* (26), 7017.
(35) Mantina, M.; Chamberlin, A. C.; Valero, R.; Cramer, C. J.; Truhlar, D. G. *J. Phys. Chem. A* **2009**, *113*, 5806.
(36) Atwood, J. L.; Smith, K. D. *J. Am. Chem. Soc.* **1974**, *96* (4), 994.
(37) Deacon, G. B.; Forsyth, C. M.; Junk, P. C. *J. Organomet. Chem.* **2000**, *607*, 112.
(38) Hitzbleck, J.; Deacon, G. B.; Ruhlandt-Senge, K. *Angew. Chem., Int. Ed.* **2004**, *43* (39), 5218.
(39) Zuniga, M. F.; Deacon, G. B.; Ruhlandt-Senge, K. *Chem.—Eur. J.* **2007**, *13*, 1921.
(40) Zuniga, M. F.; Kreutzer, J.; Ruhlandt-Senge, K. *Inorg. Chem.* **2007**, *46*, 10400.
(41) Zuniga, M. F.; Deacon, G. B.; Ruhlandt-Senge, K. *Inorg. Chem.* **2008**, *47*, 4669.
(42) Jacobs, H.; Hadenfeld, C. *Z. Anorg. Allg. Chem.* **1975**, *418*, 132.
(43) O'Brien, A. Y.; Hitzbleck, J.; Torvisco, A.; Deacon, G. B.; Ruhlandt-Senge, K. *Eur. J. Inorg. Chem.* **2008**, *1*, 172.
(44) Gilman, H.; Gorsich, R. D. *J. Am. Chem. Soc.* **1955**, *77* (11), 3134.
(45) Eberhardt, G. C.; Butte, W. A. *J. Org. Chem.* **1974**, *29*, 2928.
(46) Hage, M.; Ogle, C. A.; Rathman, T. L.; Hubbard, J. L. *Main Group Met. Chem.* **1998**, *21* (12), 777.
(47) Beno, M. A.; Hope, H.; Olmstead, M. M.; Power, P. P. *Organometallics* **1985**, *4*, 2117.
(48) Müller, G.; Lutz, M.; Wald-Kircher, M. *Acta Crystallogr., Sect. C* **1996**, *C52*, 1182.
(49) Patterman, S. P.; Karle, I. L.; Stucky, G. D. *J. Am. Chem. Soc.* **1970**, *92* (5), 1150.
(50) Tatic, T.; Hermann, S.; John, M.; Loquet, A.; Lange, A.; Stalke, D. *Angew. Chem., Int. Ed.* **2011**, *50*, 6666.
(51) Zarges, W.; Marsch, M.; Harms, K.; Boche, G. *Chem. Ber.* **1989**, *122*, 2303.
(52) Arnold, J.; Knapp, V.; Schmidt, J. A. R.; Shafir, A. *J. Chem. Soc., Dalton Trans.* **2002**, 3273.
(53) Davidson, M. G.; Garcia-Vivo, D.; Kennedy, A. R.; Mulvey, R. E.; Robertson, S. D. *Chem.—Eur. J.* **2011**, *17*, 3364.
(54) Bailey, P. J.; Coxall, R. A.; Dick, C. M.; Fabre, S.; Henderson, L. C.; Herber, C.; Liddle, S. T.; Loroño-González, D.; Parkin, A.; Parsons, S. *Chem.—Eur. J.* **2003**, *9*, 4820.
(55) Schade, C.; Schleyer, P. v. R.; Dietrich, H.; Mahdi, W. *J. Am. Chem. Soc.* **1986**, *108* (9), 2484.
(56) Corbelin, S.; Lorenzen, N. P.; Kopf, J.; Weiss, E. *J. Organomet. Chem.* **1991**, *415*, 293.
(57) Harder, S.; Müller, S.; Hübner, E. *Organometallics* **2004**, *23*, 178.
(58) Westerhausen, M.; Schwarz, W. *Z. Naturforsch., Sect. B: Chem. Sci.* **1998**, *53* (5/6), 623.
(59) Hoffmann, D.; Bauer, W.; Hampel, F.; van Eikema Hommes, N. J. R.; Schleyer, P. v. R.; Otto, P.; Pieper, U.; Stalke, D.; Wright, D. S.; Snaith, R. *J. Am. Chem. Soc.* **1994**, *116* (2), 528.
(60) Schlosser, M. *Pure Appl. Chem.* **1988**, *60*, 1627.
(61) Alexander, J. S.; Ruhlandt-Senge, K. *Chem.—Eur. J.* **2004**, *10*, 1274.
(62) Alexander, J. S.; Ruhlandt-Senge, K. *Angew. Chem., Int. Ed.* **2001**, *40* (14), 2658.
(63) Alexander, J. S.; Ruhlandt-Senge, K. *Eur. J. Inorg. Chem.* **2002**, *11*, 2761.
(64) Guino-o, M. A.; Torvisco, A.; Teng, W.; Ruhlandt-Senge, K. *XXXXX* **2011**in press.
(65) Alexander, J. S.; Ruhlandt-Senge, K.; Hope, H. *Organometallics* **2003**, *22*, 4933.
(66) Guino-o, M. A.; Alexander, J. S.; McKee, M. L.; Hope, H.; Englich, U.; Ruhlandt-Senge, K. *Chem.—Eur. J.* **2009**, *15*, 11842.
(67) Torvisco, A.; O'Brien, A. Y.; Ruhlandt-Senge, K. *Coord. Chem. Rev.* **2011**, *255*, 1268.
(68) West, P.; Woodville, M. C. U.S. Patent 3718703, 1973.
(69) De Groof, B.; Van Beylen, M.; Szwarc, M. *Macromolecules* **1975**, *8*, 396.
(70) De Groof, B.; Mortier, W.; Van Beylen, M.; Swarc, M. *Macromolecules* **1977**, *10*, 598.
(71) Arest-Yakubich, A. A. *Russ. Chem. Rev.* **1981**, *50*, 601.
(72) Nakhmanovich, B. I.; Arest-Yakubovich, A. A. *Dokl. Phys. Chem.* **1976**, *228*, 426.
(73) Weeber, A.; Harder, S.; Brintzinger, H. H.; Knoll, K. *Organometallics* **2000**, *19*, 1325.
(74) Guino-o, M. A.; Campana, C. F.; Ruhlandt-Senge, K. *Chem. Commun.* **2007**, 1692.
(75) Weiss, E. *Angew. Chem., Int. Ed. Engl.* **1993**, *32* (11), 1501.
(76) Mulvey, R. E. *Chem. Commun.* **2001**, 1049.
(77) Hitchcock, P. B.; Huang, Q.; Lappert, M. F.; Wei, X.-H.; Zhou, M. *Dalton Trans.* **2006**, 2991.
(78) Davies, R. P. *Inorg. Chem. Commun.* **2000**, *3*, 13.
(79) Kennedy, A. R.; Mulvey, R. E.; Rowlings, R. B. *J. Organomet. Chem.* **2002**, *648*, 288.
(80) He, X.; Noll, B. C.; Beatty, A.; Mulvey, R. E.; Henderson, K. W. *J. Am. Chem. Soc.* **2004**, *126*, 7444.
(81) Maudez, W.; Häussinger, D.; Fromm, K. M. *Z. Anorg. Allg. Chem.* **2006**, *632*, 2295.
(82) Coan, P. S.; Streib, W. E.; Caulton, K. G. *Inorg. Chem.* **1991**, *30*, 5019.
(83) Bock, H.; Hauck, T.; Näther, C.; Rösch, N.; Staufer, M.; Häberlen, O. D. *Angew. Chem., Int. Ed. Engl.* **1995**, *34*, 1353.
(84) Fromm, K. M.; Gueneau, E. D.; Goesmann, H. *Chem. Commun.* **2000**, 2187.
(85) Fromm, K. M. *Dalton Trans.* **2006**, 5103.
(86) Frankland, A. D.; Lappert, M. F. *J. Chem. Soc., Dalton Trans.* **1996**, 4151.
(87) Hitchcock, P. B.; Khvostov, A. V.; Lappert, M. F. *J. Organomet. Chem.* **2002**, *663*, 263.
(88) Kinsley, S. A.; Streitwieser, J. A; Zalkin, A. *Organometallics* **1985**, *4*, 52.
(89) Fischer, R.; Görls, H.; Westerhausen, M. *Organometallics* **2007**, *26*, 3269.
(90) Hevia, E.; Henderson, K. W.; Kennedy, A. R.; Mulvey, R. E. *Organometallics* **2006**, *25*, 1778.
(91) Westerhausen, M.; Gückel, C.; Habereder, T.; Vogt, M.; Warchold, M.; Nöth, H. *Organometallics* **2001**, *20*, 893.
(92) Knapp, V.; Müller, G. *Angew. Chem., Int. Ed.* **2001**, *40* (1), 183.
(93) Schubert, B.; Weiss, E. *Chem. Ber.* **1984**, *117*, 366.
(94) Baker, D. R.; Clegg, W.; Horsburgh, L.; Mulvey, R. E. *Organometallics* **1994**, *13*, 4170.
(95) Engelhardt, L. M.; Leung, W.-P.; Raston, C. L.; Salem, G.; Twiss, P.; White, A. H. *J. Chem. Soc., Dalton Trans.* **1988**, 2403.
(96) Bildmann, U. J.; Müller, G. *Organometallics* **2001**, *20*, 1689.
(97) Feil, F.; Harder, S. *Organometallics* **2001**, *20*, 4616.

(98) Harder, S.; Feil, F.; Knoll, K. *Angew. Chem., Int. Ed.* **2001**, *40* (22), 4261.
(99) Harder, S.; Feil, F.; Weeber, A. *Organometallics* **2001**, *20*, 1044.
(100) Harder, S.; Feil, F. *Organometallics* **2002**, *21*, 2268.
(101) Piesik, D. F.-J.; Häbe, K.; Harder, S. *Eur. J. Inorg. Chem.* **2007**, *36*, 5652.
(102) Bradley, D. C.; Hursthouse, M. B.; Ibrahim, A. A.; Abdul, A. M.; Motevalli, R.; Moseler, R.; Powell, H.; Runnacles, J. D.; Sullivan, A. C. *Polyhedron* **1990**, *9*, 2459.
(103) Alexander, J. S.; Allis, D. G.; Teng, W.; Ruhlandt-Senge, K. *Chem.—Eur. J.* **2007**, *13*, 9899.
(104) Olmstead, M. M.; Power, P. P. *J. Am. Chem. Soc.* **1985**, *107* (7), 2174.
(105) Clayden, J. *Organolithiums: Selectivity for Synthesis*; Pergamon: Amsterdam, The Netherlands, 2002.
(106) Schumann, H.; Freckmann, D. M. M.; Dechert, S. *Organometallics* **2006**, *25*, 2696.
(107) Jenkins, D. M.; Teng, W.; Englich, U.; Ruhlandt-Senge, K. *Organometallics* **2001**, *20*, 4600.
(108) Uhlig, F.; Hummeltenberg, R. *J. Organomet. Chem.* **1993**, *452*, C9.
(109) Uhlig, F.; Ruhlandt-Senge, K.; Hassler, K.; Englich, U. *Inorg. Chem.* **1998**, *37*, 3532.
(110) Marschner, C. *Eur. J. Inorg. Chem.* **1998**, *2*, 221.
(111) Hill, M. S.; Hitchcock, P. B. *Organometallics* **2002**, *21*, 220.
(112) Alexander, J. S.; Allis, D. G.; Hudson, B. S.; Ruhlandt-Senge, K. *J. Am. Chem. Soc.* **2003**, *125* (49), 15002.
(113) Englich, U.; Ruhlant-Senge, K. *Coord. Chem. Rev.* **2000**, *210*, 135.
(114) Byrne, L. T.; Engelhardt, L. M.; Jacobsen, G. E.; Leung, W.-P.; Papasergio, R. I.; Raston, C. L.; Skelton, W. B.; Twiss, P.; White, A. H. *J. Chem. Soc., Dalton Trans.* **1989**, 105.
(115) Clegg, W.; Izod, K.; McFarlane, W.; O'Shaughnessy, P. *Organometallics* **1999**, *18*, 3950.
(116) Decken, A.; Cowley, A. H. *J. Organomet. Chem.* **1996**, *509*, 135.
(117) Winkler, M.; Lutz, M.; Müller, G. *Angew. Chem.* **1994**, *106* (22), 2372.
(118) Shi, H.-P.; Liu, D.-S.; Huang, S.-P. *Acta Crystallogr., Sect. C* **2004**, *C60*, 107.
(119) Boche, G.; Decher, G.; Etzrodt, H.; Dietrich, H.; Mahdi, W.; Kos, A. J.; Schleyer, P. v. R. *Chem. Commun.* **1984**, 1493.
(120) Lappert, M. F.; Raston, C. L.; Skelton, W. B.; White, A. H. *Chem. Commun.* **1982**, 14.
(121) Leung, W.-P.; Raston, C. L.; Skelton, W. B.; White, A. H. *J. Chem. Soc., Dalton Trans.* **1984**, 1801.
(122) Engelhardt, L. M.; Leung, W.-P.; Raston, C. L.; Twiss, P.; White, A. H. *J. Chem. Soc., Dalton Trans.* **1984**, 321.
(123) Zarges, W.; Marsch, M.; Harms, K.; Koch, W.; Frenking, G.; Boche, G. *Chem. Ber.* **1991**, *124*, 543.
(124) Schumann, H.; Freckmann, D. M. M.; Dechert, S. *Z. Anorg. Allg. Chem.* **2008**, *634*, 1334.
(125) Colgan, D.; Papasergio, R. I.; Raston, C. L.; White, A. H. *J. Chem. Soc., Chem. Commun.* **1984**, 1708.
(126) Engelhardt, L. M.; Leung, W.-P.; Raston, C. L.; White, A. H. *J. Chem. Soc., Dalton Trans.* **1985**, 337.
(127) Fraenkel, G.; Duncan, J. H.; Martin, K.; Wang, J. *J. Am. Chem. Soc.* **1999**, *121* (45), 10538.
(128) Hacker, R.; Schleyer, P. v. R.; Reber, G.; Müller, G.; Brandsma, L. *J. Organomet. Chem.* **1986**, *316*, C4.
(129) Hill, M. S.; Hitchcock, P. B. *J. Organomet. Chem.* **2002**, *664*, 182.
(130) Feil, F.; Müller, C.; Harder, S. *J. Organomet. Chem.* **2003**, *683*, 56.
(131) Nagel, U.; Nedden, H. G. *Chem. Ber.* **1997**, *130*, 535.
(132) Gardiner, M. G.; Raston, C. L.; Viebrock, H. *Chem. Commun.* **1996**, 1795.
(133) Bartlett, R. A.; Dias, H. V. R.; Power, P. P. *J. Organomet. Chem.* **1988**, *341*, 1.
(134) Brooks, J. J.; Stucky, G. D. *J. Am. Chem. Soc.* **1972**, *94* (21), 7333.
(135) Köster, H.; Weiss, E. *J. Organomet. Chem.* **1979**, *168*, 273.
(136) Fernández, I.; Martínez-Viviente, E.; Breher, F.; Pregosin, P. S. *Chem.—Eur. J.* **2005**, *11*, 1495.
(137) Viebrock, H.; Panther, T.; Behrens, U.; Weiss, E. *J. Organomet. Chem.* **1995**, *491*, 19.
(138) Hoffmann, D.; Bauer, W.; Schleyer, P. v. R. *Organometallics* **1993**, *12*, 1193.
(139) Ma, J. C.; Dougherty, D. A. *Chem. Rev.* **1997**, *97* (5), 1303.
(140) Dougherty, D. A. *Science* **1996**, *271*, 163.
(141) Gokel, G. W.; De Wall, S. L.; Meadows, E. S. *Eur. J. Org. Chem.* **2000**, *17*, 2967.
(142) Fukin, G. K.; Lindeman, S. V.; Kochi, J. K. *J. Am. Chem. Soc.* **2002**, *124* (28), 8329.
(143) Cabarcos, O. M.; Weinheimer, C. J.; Lisya, J. M. *J. Chem. Phys.* **1998**, *108* (13), 5151.
(144) Cabarcos, O. M.; Weinheimer, C. J.; Lisya, J. M. *J. Chem. Phys.* **1999**, *110* (17), 8429.
(145) Bock, H.; Hauck, T.; Näther, C. *Z. Kristallogr.* **1998**, *213* (3), 174.
(146) Chadwick, S.; Englich, U.; Noll, B.; Ruhlandt-Senge, K. *Inorg. Chem.* **1998**, *37* (18), 4718.
(147) Harder, S.; Feil, F.; Repo, T. *Chem.—Eur. J.* **2002**, *8*, 1991.
(148) Engelhardt, L. M.; Harvey, S.; Raston, C. L.; White, A. H. *J. Organomet. Chem.* **1988**, *341*, 39.
(149) Fedushkin, I. L.; Lukoyanov, A. N.; Dechert, S.; Schumann, H. *Eur. J. Inorg. Chem.* **2004**, 2421.
(150) Deacon, G. B.; Forsyth, C. M.; Jaroschik, F.; Junk, P. C.; Kay, D. L.; Maschmeyer, T.; Masters, A. F.; Wang, J.; Field, L. D. *Organometallics* **2008**, *27* (18), 4772.
(151) Verma, A.; Guino-o, M.; Gillett-Kunnath, M.; Teng, W.; Ruhlandt-Senge, K. *Z. Anorg. Allg. Chem.* **2009**, *635*, 903.
(152) Westerhausen, M.; Hartmann, M.; Makropoulos, N.; Wieneke, B.; Wieneke, M.; Schwarz, W.; Stalke, D. *Z. Naturforsch., Sect. B: Chem. Sci.* **1998**, *53* (1), 117.
(153) Vargas, W. Doctoral Dissertation, Syracuse University, Syracuse, NY, 2003.
(154) Westerhausen, M.; Schwarz, W. *Z. Anorg. Allg. Chem.* **1991**, *604*, 127.
(155) Jayaratne, K. C.; Fitts, L. S.; Hanusa, T. P.; Young, V. G., Jr. *Organometallics* **2001**, *20* (17), 3638.
(156) Leyser, N.; Schmidt, K.; Brintzinger, H.-H. *Organometallics* **1998**, *17* (11), 2155.
(157) Pieper, U.; Stalke, D. *Organometallics* **1993**, *12*, 1201.
(158) Feil, F.; Harder, S. *Organometallics* **2000**, *19*, 5010.
(159) Miravitlles, C.; Solans, X.; Germain, G.; Declercq, J. P. *J. Inclusion Phenom. Mol. Recognit. Chem.* **1985**, *3* (1), 27.
(160) Andrews, P. C.; Raston, C. L.; Roberts, B. A.; Skelton, W. B.; White, A. H. *J. Organomet. Chem.* **2006**, *691*, 3325.